

# Quantum Encoding and Analysis on Continuous Time Stochastic Process with Financial Applications

Xi-Ning Zhuang,<sup>1,2</sup> Zhao-Yun Chen,<sup>3</sup> Cheng Xue,<sup>3</sup> Yu-Chun Wu,<sup>1,4,5,3,\*</sup> and Guo-Ping Guo<sup>1,4,5,3,2,†</sup>

<sup>1</sup>CAS Key Laboratory of Quantum Information, University of Science and Technology of China, Hefei, 230026, China

<sup>2</sup>Origin Quantum Computing, Hefei, China

<sup>3</sup>Institute of Artificial Intelligence, Hefei Comprehensive National Science Center

<sup>4</sup>CAS Center for Excellence and Synergistic Innovation Center in Quantum Information and Quantum Physics, University of Science and Technology of China, Hefei, 230026, China

<sup>5</sup>Hefei National Laboratory, University of Science and Technology of China, Hefei 230088, China

To model the stochastic world on continuous time is an essential but challenging problem. We establish the algorithm framework of quantum continuous time stochastic process to solve this problem. Two procedures are handled to achieve quantum speed-up, the data loading, and the information extraction. The data loading procedure's space and time complexities are both reduced exponentially on the key parameter, and this procedure can be employed as an efficient input module for other quantum algorithms. The information extraction procedure admits a further quadratic acceleration, which extends the quantum Monte Carlo method. Because of its flexibility and versatility, this framework can be utilized within a wide range of applications involving finance, statistics, physics, and time series analysis. Two examples of option pricing in the Merton Jump Diffusion Model and ruin probability computing in the Collective Risk Model are given to illustrate the ability to capture extreme market events and history-dependent information.

## I. INTRODUCTION

The continuous time stochastic process (CTSP), encompassing many well-known stochastic processes from *Poisson point process*, *compound Poisson process*, *Lévy process*, *continuous Markov process*, to doubly stochastic *Cox process*, is an essential and fundamental mathematical instrument to model the stochastic world defined on continuous time variables, and it can be applied to a wide range of fields, including but not limited to finance, physics, statistics, and biology [1–5]. However, due to its continuous path, CTSP is believed to be much more complicated than its discrete counterpart: For most practical problems, there is no analytic solution or explicit formula to the underlying stochastic differential equations and quantities. Furthermore, unexpectedly large storage and computation resources are consumed when applying numerical methods such as Monte Carlo simulation because the sampling space grows exponentially as time slices go thinner [6, 7].

The development of quantum processors [8–10] and algorithms [11–18] has revealed that quantum computation has great potential beyond classical computers. Thus it would be one powerful tool to solve the above challenging problems. However, there are still two fundamental challenges to overcome when implementing the storage and analysis of CTSP with a quantum computer.

The first challenge is the data loading of CTSP: As a common and primary bottleneck faced by quantum machine learning and many other algorithms[19], the state preparation problem has been studied and discussed in

many works [20–22]. Quantum analog simulators are proposed to predict the future of a specified class of CTSP named renewal process with less past information, and a perhaps unbounded memory requirement reduction is made in [23–25]. The quantum advantage in simulating stochastic process is further discussed in [26]. Nevertheless, those works have not solve the CTSP preparation problem for three reasons: The information is not digital-encoded, so the analysis, such as quantum Monte Carlo is not easy to implement. Moreover, the type of CTSP is restricted to the renewal process. Furthermore, the storage of the whole path is absent, leading to crucial practical problems for financial engineering, quantitative trading, and many other path-dependent scenarios.

The second challenging problem is the information extraction of CTSP. Quantum Monte Carlo simulation, which means to generate random paths and compute the expectation of desired value, has been proven to make a quadratic quantum speed up on computing the final value of discrete sampling paths [27–32]. Also a weightless summation of discrete paths aiming at Asian-type option pricing is proposed in work [29]. However, the Monte Carlo simulation of CTSP, including the expectation of a weighted integral on the CTSP paths and the extraction of history-sensitive information (such as the first-hitting time problem), are left unsolved.

In this work, we establish a framework to solve the problems of state preparation and information extraction of quantum continuous time stochastic process (QCTSP). Two representations encoding general QCTSP are introduced. The corresponding state preparation method is developed to prepare the QCTSP with less qubit number requirement, higher flexibility, and more sensitivity to discontinuous jumps that are important to model extreme market events such as *flash crash*. An observation of the CTSP holding time is made, induc-

\* wuyuchun@ustc.edu.cn

† gpguo@ustc.edu.cn

ing further reductions in the circuit depth and the gate complexity of QCTSP. Specific quantum circuits are designed for most of the often-used CTSPs with exponential reduction of both qubit number and circuit depth on the key parameter of QCTSP named holding time  $\tau_{avg}$  (as summarized in table II). As for the information extraction problem of QCTSP, the weightless integral and the arbitrary time-weighted integral of the QCTSP can be efficiently evaluated by computing the summation of directed areas. Furthermore, this method enables the quantum Monte Carlo framework to extend to the continuous-time regime, admitting a quadratic quantum speed up. Moreover, by introducing a sequence of flag qubits, our method can extract the history-sensitive information that is essential and indispensable for quantitative finance, path-dependent option pricing, and actuarial science, to cite but a few examples.

Applications of computing the European type option price in the *Merton Jump Diffusion Model* and the ruin probability in the *Collective Risk Model* are given. The first application of evaluating a European-type option has been studied in previous work [28–30, 32], while our method takes the more practical situation of the discontinuous price movement into consideration, and the simulation result is consistent with the *Merton* formula. The second application of computing the ruin probability opens up new opportunities in the area of insurance as being the first time that quantum computing has been introduced into insurance mathematics up to known, illustrating the great potential power of QCTSP.

In addition to the theoretical importance and rich applicability of QCTSP mentioned above, our work also benefits from its low requirement of input data and circuit connectivity. It can be utilized as an input without quantum random access memory (qRAM) [33–35], partly solving the input problem that quantum machine learning and many other quantum algorithms are confronted with. Simultaneously, an indicator is given in this work to characterize not only the preparation procedure’s complexity but the circuit connectivity as well.

The structure of this article is as follows: Given the mathematical notations for readability and the formal problem statement, the main framework of QCTSP is sketched in section II. The main results of state preparation and information extraction are organized in section III and section IV, respectively. Followed by two applications of option pricing and insurance mathematics in section V, the discussion, together with an introduction of future work, is given in section VI. The detailed construction of specific modified subcircuits and proofs can be found in the APPENDIX.

## II. QUANTUM CONTINUOUS TIME STOCHASTIC PROCESS

The mathematical notation is given in the first subsection, followed by the formal definition of CTSP and

TABLE I. Mathematical Symbols

Notation	Nomenclature
$\mathbb{P}$	The probability.
$\Omega$	Space of CTSP
$\tilde{\Omega}_n$	Space of CTSP of $n$ deterministic pieces
$\mathcal{S}$	Space of states of point
$S$	the size of the Space of states $S =  \mathcal{S} $
$\mathbb{Z}_S$	The set of index $\{1, \dots, S\}$
$T$	Time slices
$\mathbb{Z}_T$	The set of time $\{1, \dots, T\}$
$n$	Number of Pieces
$X(t)$	A CTSP
$X_j$	The $j^{\text{th}}$ piece’s value variable
$x_{j,k_j}$	A realization of $X_j$ , taking the $k_j \in \mathcal{S}$ index, in path
$Y_j$	The $j^{\text{th}}$ piece’s increment
$\tau_j$	The $j^{\text{th}}$ piece’s holding time
$t_j$	A realization of $\tau_j$ in path
$T_j$	The $j^{\text{th}}$ piece’s cumulative time
$\mathcal{ML}(X)$	The memory length of $X(t)$

the two representations of QCTSP. Then the core problems of state preparation and information extraction of QCTSP are stated. A brief framework of our QCTSP is described at the end of this section.

### A. Notation

Formally speaking, given the mathematical symbols in table I and a discrete state space or its discretization  $\mathcal{S} (S = |\mathcal{S}| \in \mathbb{N}_+)$ , a CTSP can be defined as

**Definition 1. (Continuous Time Stochastic Process)** Given a discrete space  $\mathcal{S}$ , A continuous time stochastic process  $\{X(t) : t \geq 0\}$  is a stochastic process defined on the continuous variable  $t$ , where for each  $t_0$ , the state  $X(t_0) \in \mathcal{S}$  is a stochastic variable whose possibility distribution is determined by  $\mathbb{P}[X(t_0)] = \mathbb{P}[X(t_0)|X(t) : 0 \leq t < t_0]$ .

For a given CTSP, the most significant distinction from the discrete case is the uncountable dimensional space of continuous sample paths denoted by  $\Omega$ . As the time slices become thinner, the sample space becomes a disaster for both theoretical analysis and simulation. Henceforth, the reduced space  $\tilde{\Omega}_n$  consists of those paths that can be divided into finite  $n \in \mathbb{N}_+$  in-variate pieces is considered, where each  $\{X(t) : t \geq 0\}$  in  $\tilde{\Omega}_n$  is a piece-wise determined random function  $X(t) = X_j$  for  $T_{j-1} \leq t < T_j$  with  $T_0 = 0$ .

Thus the  $j^{\text{th}}$  piece can be recorded as a pair of random variables  $(X_j, \tau_j)$ , where  $X_j \in \mathcal{S}$  is a discrete random variable that denotes the  $j^{\text{th}}$  piece’s state, and  $\tau_j = T_j - T_{j-1} \in \mathbb{N}^+$  is a strictly positive random variable that denotes lifetime length of the  $j^{\text{th}}$  piece. In this way, the whole CTSP is encoded via a sequence of random variable pairs  $\{(X_j, \tau_j) : 1 \leq j \leq n\}$ , which will be called the

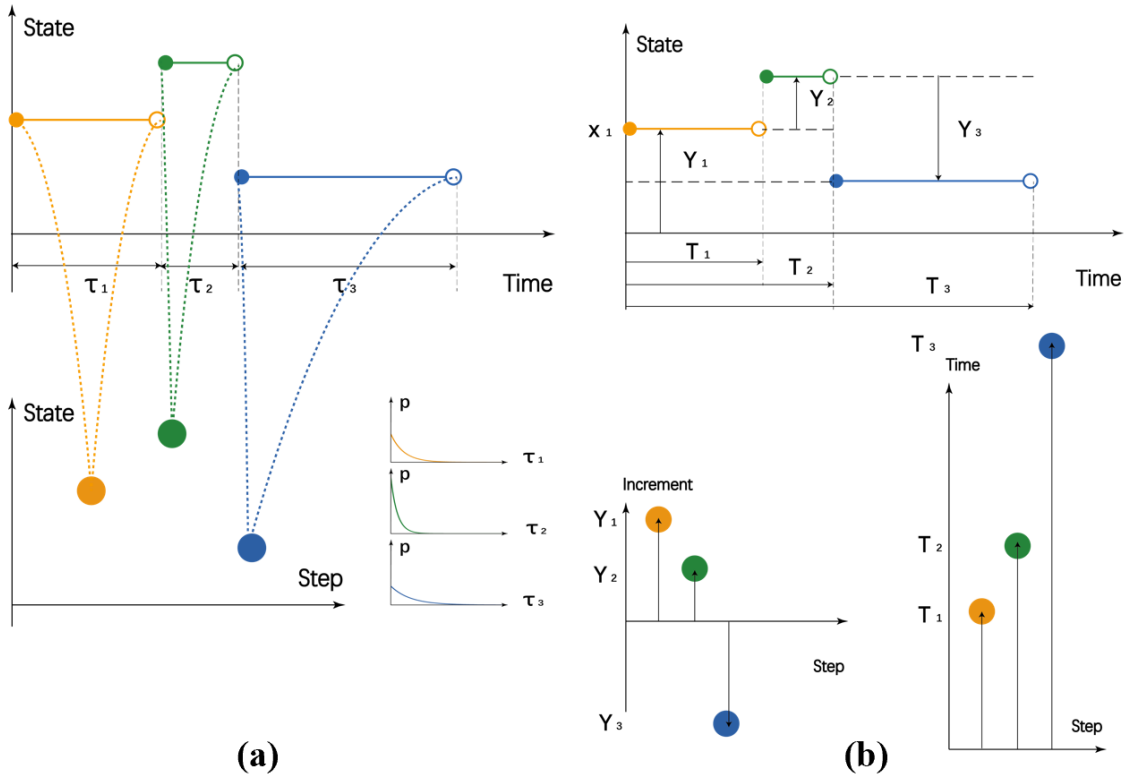


FIG. 1. **Embed a Continuous Time Stochastic Process to a pair of Discrete Stochastic Processes.** In this figure, a continuous time stochastic process is embedded into discrete stochastic processes via two different representations. (a) As shown in the left subfigure, the  $j^{\text{th}}$  in-variant piece of CTSP can be compressed into a discrete random variable  $X_j$  (denoted by the point) in the state space, together with a holding time variable  $\tau_j$  follows a given probability distribution (illustrated by a picture of the probability density function). (b) As shown in the right subfigure, the  $j^{\text{th}}$  in-variant piece of CTSP can be compressed into a discrete random variable of increment  $Y_j = X_j - X_{j-1}$  (denoted by the vertical arrow) in the state space, together with an ending time variable  $T_j$  (denoted by the horizontal arrow).

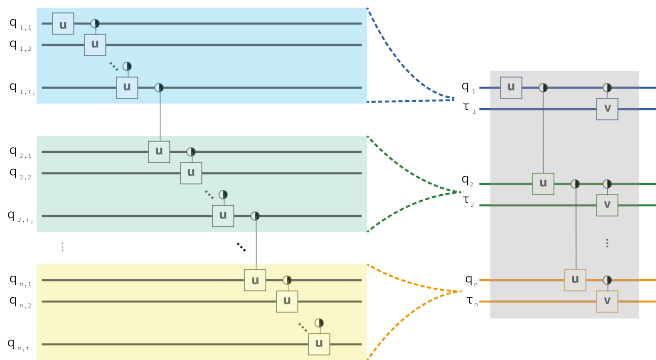


FIG. 2. **Embed a Continuous Time Stochastic Process to a pair of Discrete Stochastic Processes.** In this figure, a continuous time stochastic process is embedded into a sequence of stochastic pairs. Both the qubit number and the circuit depth is reduced as shown.

holding time representation hereafter (as illustrated in FIG. 1 (a)). More precisely, we have:

**Definition 2. (Holding Time Representation of**

**Quantum Continuous Time Stochastic Process )** Given a continuous time stochastic process  $\{X(t) : t \geq 0\}$ , the holding time representation of quantum continuous time stochastic process is a sequence of stochastic pairs  $(X_j, \tau_j)$  satisfies: (1)  $X(t) = X_j : T_{j-1} \leq t < T_j$ , (2)  $\tau_j = T_j - T_{j-1}$ , and (3)  $\mathbb{P}[X_j, \tau_j] = \mathbb{P}[X_j, \tau_j | X_{j'}, \tau_{j'} : 1 \leq j' < j]$ .

An alternative method named *increment representation* to encode a CTSP is to consider an equivalent sequence of random variable pairs  $\{(Y_j, T_j) : 1 \leq j \leq n\}$  where  $Y_1 = X_1$  and  $Y_j = X_j - X_{j-1}$  are the increments of the CTSP (as illustrated in FIG. 1 (b)):

**Definition 3. (Increment Representation of Quantum Continuous Time Stochastic Process )** Given a continuous time stochastic process  $\{X(t) : t \geq 0\}$ , the increment representation of quantum continuous time stochastic process is a sequence of stochastic pairs  $(Y_j, T_j)$  satisfies: (1)  $X(t) = X_j : T_{j-1} \leq t < T_j$ , (2)  $Y_j = X_j - X_{j-1}$ , and (3)  $\mathbb{P}[Y_j, T_j] = \mathbb{P}[Y_j, T_j | Y_{j'}, T_{j'} : 1 \leq j' < j]$ .

Instead of the uniform sampling method, these two encoding methods benefit from the reduction of qubit num-

ber (as shown in Fig. 2), as well as the ability to capture randomly happened discontinuous jumps (as circled in Fig. 4 (a) and Fig. 6 (a)). These two equivalent representations are proposed simultaneously to efficiently compute path-dependent and history-sensitive information, as stated later in section IV.

## B. Problem statement

In this paper, the QCTSP is assumed to be stored in three registers named the index register  $|0\rangle_{index}$ , the data register  $|0\rangle_{data}$  and the time register  $|0\rangle_{time}$  for the storage of the index sequence  $\{k_j\}$ , the path sequence  $\{X_j\}$  and the holding time sequence  $\{\tau_j\}$ , respectively. Then the QCTSP state lying in the Hilbert space  $\mathcal{H}_{k,x} \otimes \mathcal{H}_t = (\mathbb{Z}_S \mathbb{C} \mathbb{Z}_T)^{\otimes n}$  can be represented as

$$|\psi\rangle = \sum_{\mathbf{k}, \mathbf{t} \in \mathbb{Z}_S^n \otimes \mathbb{Z}_T^n} p(\mathbf{k}, \mathbf{t}) |\mathbf{k}, \mathbf{x}(\mathbf{k}), \mathbf{t}\rangle, \quad (1)$$

where  $\mathbf{k} = (k_1, \dots, k_n)^\top \in \mathbb{Z}_S^n$  satisfies

$$x_{j,k_j} = x(k_j) : 1 \leq j \leq n, 1 \leq k_j \leq |S|$$

and means that the  $j^{th}$  piece takes the  $k_j^{th}$  value in the state space  $\mathcal{S}$ , and  $\mathbf{t} = (t_1, \dots, t_n)^\top \in \mathbb{Z}_T^n$  where  $1 \leq t_j \leq T$  is a realization of the sequence  $(\tau_1, \dots, \tau_n)$  and means that the  $j^{th}$  piece stays for  $t_j$  time slices bounded by  $T$ . According to Definition 1, for each time piece, the current pair  $(X_j, \tau_j)$  is derived from the past pieces  $\{(X_{j'}, \tau_{j'}) : 1 \leq j' \leq j-1\}$  with the possibility amplitude  $p(\mathbf{k}, \mathbf{t})$  satisfies

$$\begin{aligned} p(\mathbf{k}, \mathbf{t}) &= p(X_1 = x(k_1)) \\ &\times p(\tau_1 = t_1 | X_1 = x(k_1)) \\ &\times \prod_{j=2}^n p(X_j = x(k_j) | X_{j'}, \tau_{j'} = x(k_{j'}), t_{j'} : 1 \leq j' < j) \\ &\times \prod_{j=2}^n p(\tau_j = t_j | X_{j'}, \tau_{j'} = x(k_{j'}), t_{j'} : 1 \leq j' < j \\ &\text{and } X_j = x(k_j)). \end{aligned} \quad (2)$$

And the possibility amplitudes also satisfy

$$\sum_{\mathbf{k}, \mathbf{t}} p^2(\mathbf{k}, \mathbf{t}) = 1. \quad (3)$$

Given a CTSP as defined in Definition 1, our first goal is to derive the corresponding QCTSP Eq.(1) encoded by Definition 2 and 3. More formally, the problem is defined as follows:

### Problem 1: QCTSP Preparation (*QCTSP-P*)

**Input:** A CTSP defined in Definition 1 and three registers  $|0\rangle_{index} |0\rangle_{data} |0\rangle_{time}$

**Question:** Is there a procedure, that is, a unitary operator  $\mathcal{U}$  acting on the registers such that  $\mathcal{U} |0\rangle_{index} |0\rangle_{data} |0\rangle_{time} = \sum_{\mathbf{k}, \mathbf{t} \in \mathbb{Z}_S^n \otimes \mathbb{Z}_T^n} p(\mathbf{k}, \mathbf{t}) |\mathbf{k}, \mathbf{x}(\mathbf{k}), \mathbf{t}\rangle$  and the possibility amplitude  $p(\mathbf{k}, \mathbf{t})$  satisfies Eq.(2) and Eq.(3)?

Supposed that a QCTSP has been prepared taking the form of Eq.(1), our second goal is to extract the information of interest, a quantity determined by the knowledge of the past path  $\{X(t) : T > t \geq 0\}$ . This problem can be stated formally as:

### Problem 2: QCTSP Extraction (*QCTSP-E*)

**Input:** A QCTSP defined as Eq.(2) and a quantity  $\mathcal{Q}$  determined by it.

**Question:** Is there a procedure, that is, a unitary operator  $\mathcal{V}$  acting on the QCTSP such that  $\mathcal{V} |\psi\rangle$  is the desired quantity  $\mathcal{Q}(\{X(t) : T > t \geq 0\})$ ?

AS there are many classes of QCTSP to be prepared, together with many quantities of interest, the detailed quantum algorithms are expounded in section III and section IV, respectively. And a brief framework illustrating the basic idea is as follows.

## C. Framework

The problem of modeling and analyzing the paths of QCTSP via a quantum processor can be divided into two main steps: Encode and prepare the QCTSP, and then decode and analyze the QCTSP.

There are prominent challenges to overcome when we try to solve the *QCTSP-P* problem. Intuitively, the complexity of the *QCTSP-P* problem is determined by the number of pieces  $n$ , the average holding time  $\tau_{avg}$ , and the intrinsic evolution complexity. The compressed encoding method appears to be natural and simple, and leads to reductions in the qubit number and the circuit depth (as illustrated in FIG. 2). By introducing the indicator *memory length* to depict the evolutionary complexity of CTSP, we first study the simplest case of memory-less process. An interesting observation of the memory-less process holding time is made, and this induces a constant circuit depth. As the memory length increases, the underlying QCTSP turns to be more complicated (shown in FIG. 3) while the property of the holding time still works: Specific types of QCTSP can be prepared efficiently (see FIG. 4, FIG. 5, and FIG. 6), and the detailed construction and the corresponding proofs are given in section III and Appendix B, respectively. The qubit number is reduced from  $O(T \ln S) = O(n\tau_{avg} \ln S)$  of the uniform sampling method to  $O(n \ln(\tau_{avg} S))$  of the QCTSP method, making an exponential reduction on the parameter  $\tau_{avg}$ . And the circuit depth is optimized from



$O(T \ln nS) = O(n\tau_{avg} \ln(nS\tau_{avg}))$  of the uniform sampling method to  $O(n \ln(nS))$  of the QCTSP method, also making an exponential reduction of qubit number on the parameter  $\tau_{avg}$ . The results of state preparation are summarized in table II.

The even more challenging *QCTSP-E* problem is to efficiently decode and extract information from QCTSP so that the quantum speed-up on preparation will not be diminished. By a controlled rotation gate-based Riemann summation of rectangles (as illustrated in FIG. 7 (a) and FIG. 7 (c)), the weightless summation of a discrete path can be extended to the time integral of a continuous path. In addition, a parallel coordinate transformation can be implemented to achieve a path-dependent weighted integral (as illustrated in FIG. 7 (b), FIG. 7 (d) and FIG. 7 (e)). Furthermore, benefited from our encoding and extracting method, the discontinuous jumps and transitions can be detected and modeled more precisely. And history-sensitive information such as first hitting time can be extracted easily as a consequence. Moreover, by introducing the amplitude estimation algorithm, the information extraction QCTSP also admits a further quadratic speed-up. The detailed construction and the corresponding proofs are given in section IV and Appendix C.

### III. STATE PREPARATION

To see why the state preparation procedure of QCTSP is non-trivial, one should be noticed that the sequence of pairs  $(X_j, \tau_j)$  can be entangled with each other for  $1 \leq j \leq n$ . Intuitively, the more the current state is influenced by past information, the more complicated gates and deeper circuits are needed. More precisely, the memory length of a given CTSP is defined as

$$\begin{aligned} \mathcal{ML}(X(t)) = \min \{n | \mathbb{P}[X(t_0) | X(t) : 0 \leq t < t_0] = \\ \mathbb{P}[X(t_0) | X(t) : t_0 - n\Delta t \leq t < t_0] \\ \text{for all } t_0 \geq n\Delta t\}, \end{aligned} \quad (4)$$

which means that the conditional probability distribution of the current time  $t_0$  is totally determined by the information in the latest  $\mathcal{ML}(X)$  time slices. Two extreme situations are compared in Fig.3: One is the worst case where the memory length  $\mathcal{ML}(X) = n$  is as long as the number of pieces. The other is the opposite case where the memory length  $\mathcal{ML}(X) = 0$ , and  $X(t)$  is said to be memory-less in this case. For the first case of the longest memory length, the present pair registers  $(X_j, \tau_j)$  should be entangled with all past time pairs of variables  $\{(X_{j'}, \tau_{j'}) : 1 \leq j' \leq j - 1\}$  together (as illustrated in FIG. 3 (a)), and this surely leads to a disaster of circuit depth and gate complexity. The second case, on the contrary, turns out to be quite simple, and we have the following result:

**Theorem 1. (Memory-less Process' Holding Time)** *Supposing that  $\{X(t) : 0 \leq t \leq T\}$  is memory-less, then the holding time  $\tau_j$  for any state  $X_j$  follows an exponential distribution  $\mathbb{P}[\tau_j \geq t] = e^{-\lambda_j t}$  with  $\lambda_j$  determined by the current state  $X_j$ . Moreover, given an  $\epsilon$  such that the cumulative density function(c.d.f)  $f$  satisfies  $\mathbb{P}[\tau_j > T] = 1 - f(T) = e^{-\lambda T} < \epsilon$ ,  $\tau_j$  can be prepared via a circuit consisting of  $\lceil \log(-\frac{1}{\lambda_j} \ln \epsilon) \rceil$  qubits with constant circuit depth 1, and the gate complexity is  $\lceil \log(-\frac{1}{\lambda_j} \ln \epsilon) \rceil$ . (see proof in Appendix B 1)*

This simple result should not be surprising since, as discussed above, the memory-less condition  $\mathcal{ML}(\tau_j) = 0$  leads to no-entanglement states and easier preparation. Following this thought, most of the often-used CTSPs have been systematically studied and efficiently prepared. The conclusion that the complexity of the state preparation of QCTSP tends to be higher as the memory length grows is further evidenced by those results summarized in table II, leaving the detailed explanation and relevant applications given as follows.

#### A. Lévy process

The first and essential family of CTSPs is the Lévy process, which is one of the most well-known families of continuous-time stochastic processes, including the Poisson process and the Wiener process (also known as Brownian motion), with applications in various fields. Formally,  $\{X(t) : t \geq 0\}$  is said to be a Lévy process if 1) the increments  $\{X(T_{j+1}) - X(T_j) : 1 \leq j \leq n\}$  are independent for any  $0 < T_1 \leq T_2 \leq \dots \leq T_n$ , and 2) stationary which means that  $X(t) - X(s)$  depends only on  $t - s$  and hence is equal in distribution to  $X(t - s)$ (as illustrated in FIG. 4 (a) and (b)). Under these assumptions, a Lévy process for the most general case can be prepared efficiently, and we have the following result:

**Theorem 2. (Upper bound of general Lévy Process' preparation)** *Supposing that  $\{X(t) : 0 < t < T\}$  is a Lévy process,  $\Delta t$  is the length of step,  $n = \frac{T}{\Delta t}$  is the length of sample path, and  $S = |\mathcal{F}|$  is the number of discretization intervals of the underlying distribution  $\mathcal{F}$ . Then the Lévy process can be prepared on  $n \log(nS)$  qubits within  $O(S + n \log(nS))$  circuit depth, and the gate complexity is thus  $O(n(S + \log(nS)))$ . (see proof in Appendix B 2)*

It should be mentioned that the preparation procedure's complexity is mainly determined by two factors: the sampling times  $n = \frac{T}{\Delta t}$  and the preparation complexity of the underlying distribution  $\mathcal{F}$ . In the most general case where compensated generalized Poisson process with countably many small jump discontinuities and Wiener process are taken into consideration, the sample space size  $S = |\mathcal{F}|$  is large and the preparation procedure of the underlying distribution  $\mathcal{F}$  may consume enormous resource of classical computation. Hence it is requisite

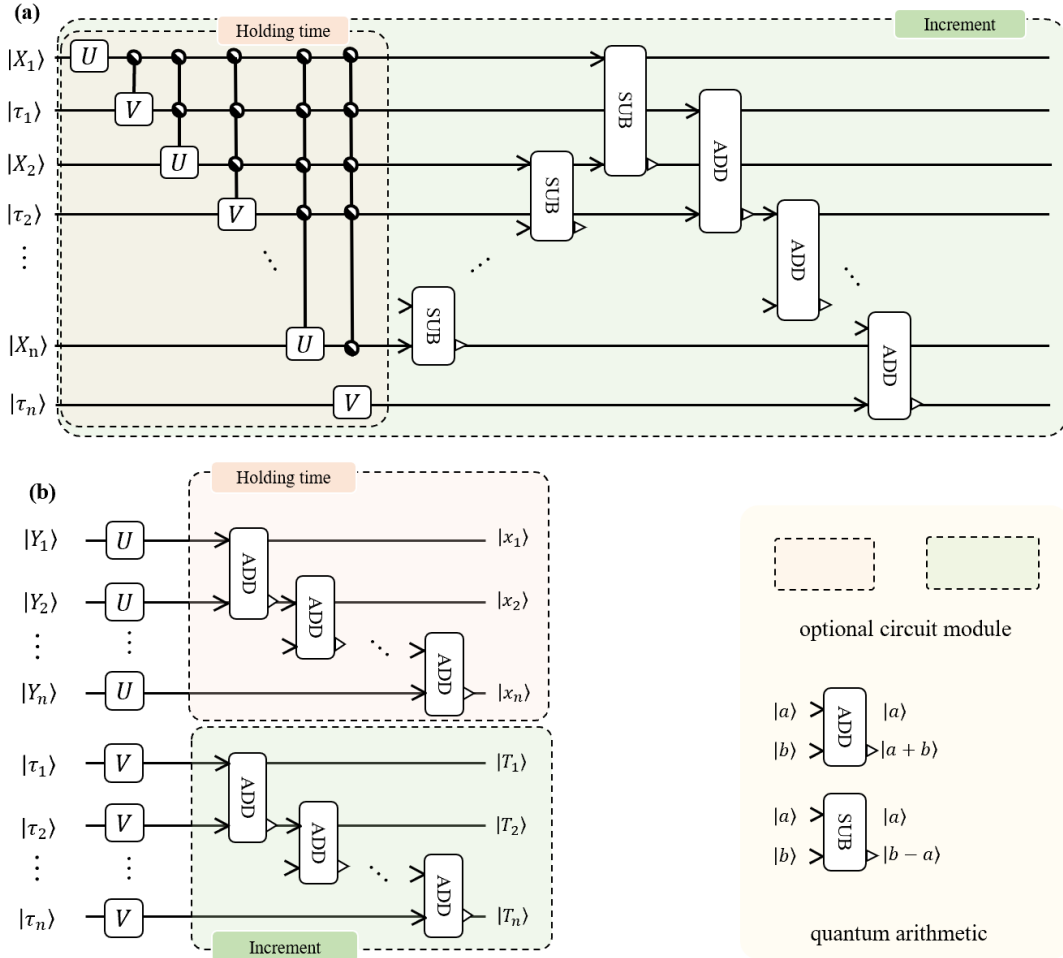


FIG. 3. **Quantum Circuits for General CTSP and compound Poisson Process** In this figure, QCTSPs of  $\mathcal{ML}(X) = n$  and *compound Poisson process* of  $\mathcal{ML}(X) = n$  are given for comparison. (a) The preparation circuit of the general CTSP is shown and the qubits storing  $X_j$  and  $\tau_j$  are highly entangled. The circuit is too complicated to simulate even for the most simple case where  $\mathcal{S} = \{0, 1\}$  and  $T = 2$ . For the  $j^{th}$  step, there are  $2^{2j-2} U_j$  operators and  $2^{2j-1} V_j$  operators. Hence the total number of unitary operators turns to be  $2^{2n} - 1$  and increases exponentially. Besides, the growth of the operator size leads to enormous challenges of gate decomposition and long-term entanglement. (b) The preparation of the Poisson process and compound Poisson process is shown. The increments  $Y_j$  and holding time  $\tau_j$  are I.I.D and can be prepared parallel through  $U$  and  $V$  operators. The alternative encoding methods can be evaluated through a sequence of add operators on  $Y_j$  and  $\tau_j$  registers in the two boxes, with respect to holding time representation and increment representation.

for one to study the more specific situations besides the upper bound given in Theorem 2, and some optimized preparation results are given below. The first example is the *Poisson point process* that plays an essential role in modeling the arrival of independent random events. More precisely, despite several equivalent definitions for different domains and applications, a CTSP is a *Poisson point process* on the positive half-line if the increment  $Y_j$  is a constant 1 and the underlying distribution of each holding time  $\tau_j$  between the events is an exponential distribution that can be efficiently prepared as shown in Theorem 1. As a direct consequence, one has:

**Corollary 3. (Poisson Point Process' preparation)** *Supposing that  $\{X(t) : 0 < t < T\}$  is a Poisson*

*process,  $\Delta t$  is the length of step,  $n = \frac{T}{\Delta t}$  is the length of sampling times, and  $\epsilon$  is the truncation of the exponential distribution  $\mathcal{F}(\lambda)$ . Then the Poisson process can be prepared on  $n \lceil \log(\frac{-n \ln \epsilon}{\lambda}) \rceil$  qubits with  $O(n \lceil \log(\frac{-n \ln \epsilon}{\lambda}) \rceil)$  control-rotation gates, and the circuit depth is  $\lceil \log n \rceil$ . (see proof in Appendix B 3)*

Another more flexible example is the *compound Poisson process* as a generalization, i.e., the jumps' random arriving time follows a Poisson process and the size of the jumps is also random with an underlying distribution  $\mathcal{G}$ . It should be noticed that each point's sampling space size  $S$  of *compound Poisson process* is usually fixed in practical, apparently different from the general Lévy process discussed above. We then get the following result with

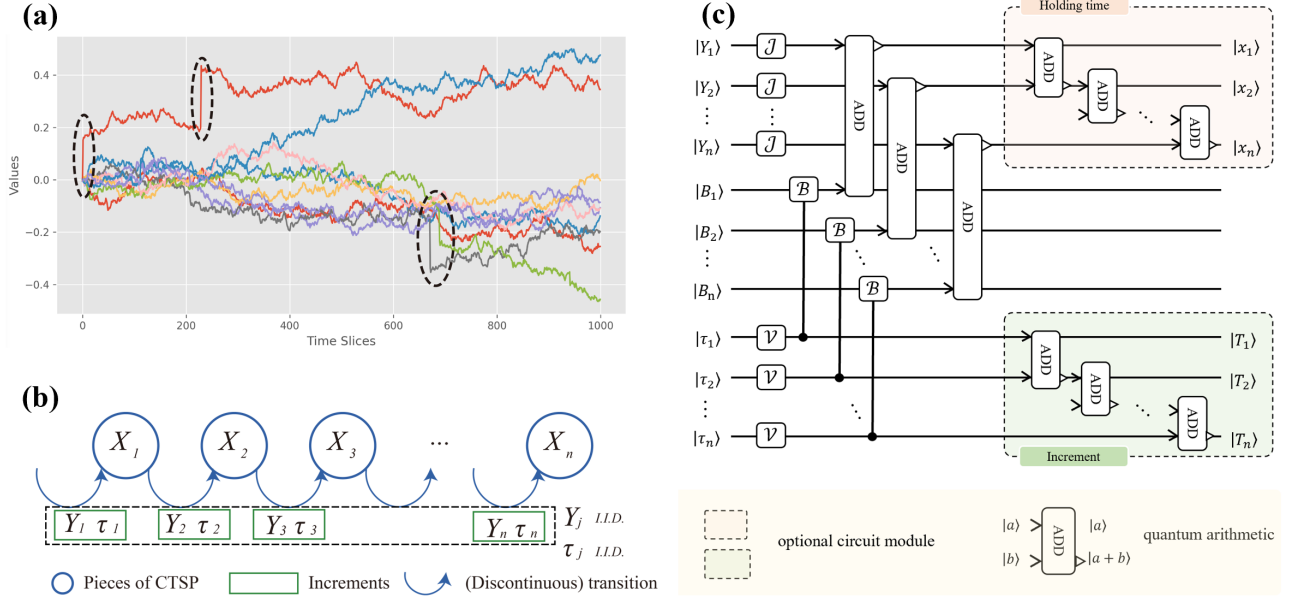


FIG. 4. **Prepare a Lévy Process.** In this figure, the preparation of a general Lévy Process is given: (a) 10 simulated Lévy process paths of 1000 steps: The intensity of discontinuous jump is  $\lambda = 1$ , and the standard deviation of jump size is  $v = 0.3$ . The standard deviation and the drift rate of the Brownian part are  $\sigma = 0.2$  and  $a = 0.02$ , respectively. As circled in the picture, discontinuous jumps happen at random timestamps that are hard for a uniform sampling method to capture. (b) A Lévy Process is embedded into discrete stochastic processes via holding time representation and increment representation encoding methods. As  $\mathcal{ML}(X) = 0$ , the corresponding stochastic pairs  $(Y_j, \tau_j)$  are I.I.D. variables. (c) The preparation of the general Lévy process is shown. The discontinuous jumps  $J_j$  and holding times  $\tau_j$  are I.I.D and can be prepared parallel through  $J$  and  $V$  operators. The Brownian motion components  $B_j$  are determined by the holding time  $\tau_j$ , and can be derived by parallel controlled- $B$  operators. The increments  $Y_j = J_j + B_j$  are then computed by parallel adder operators. It should be mentioned that operators in the grey box are implemented parallel within constant circuit depth. The alternative encoding methods can be evaluated through a sequence of adder operators on  $Y_j$  and  $\tau_j$  registers in the two boxes, with respect to holding time representation and increment representation.

some modification on the circuit(as illustrated in FIG. 3 (b)):

**Corollary 4. (Compound Poisson Process' preparation)** Suppose that  $\{X(t) : 0 < t < T\}$  is a compound Poisson process with  $n = \frac{T}{\Delta t}$  being the length of sample path,  $S$  denoting the sampling space size of each point, and  $\epsilon$  being the truncation of the exponential distribution  $\mathcal{F}(\lambda)$ , then the compound Poisson process can be prepared on  $n \lceil \log \left( \frac{-nS \ln \epsilon}{\lambda} \right) \rceil$  qubits. The circuit depth is  $S + n \lceil \log(nS) \rceil$ , and the gate complexity is  $O(n \lceil \log \left( \frac{-nS \ln \epsilon}{\lambda} \right) \rceil)$ . (see proof in Appendix B 3)

According to the Lévy-Itô decomposition, a general Lévy process can be decomposed into three components: a Brownian motion with drift  $\sigma B_t + at$ , a compound Poisson process  $Y_t$ , and a compensated generalized Poisson process  $Z_t$  as follows:

$$X_t = \sigma B_t + at + Y_t + Z_t, \quad (5)$$

where  $\sigma$  is the volatility of the Brownian motion,  $a$  is the drift rate,  $Y_t$  is the compound Poisson process of jumps larger than 1 in absolute value, and  $Z_t$  is a pure jump process with countably (infinite) many small jump

discontinuities. As  $Z_t$  contains infinitely many jumps as a zero-mean martingale, it is hard and unnecessary for preparation. One can prepare a general Lévy process without compensated parts as follows: Firstly, the sequence of exponential jumps  $J_j$  and holding times  $\tau_j$  are prepared via  $J$  and  $V$  operators, respectively. Secondly, the Brownian motions  $B_j$  are derived by Grover's state preparation method through  $B$  operators controlled by holding time  $\tau_j$ . Thirdly, an adder operator is introduced for the sum of pure jump and Brownian parts. It should be mentioned that the drift term  $at$  has been omitted since any function on this linear term can be easily translated into a function and hence well-evaluated by Theorem 7 and Theorem 8. The circuit is shown in FIG. 4 (c).

## B. Continuous Markov process

The second and more complicated family of CTSPs is the *continuous Markov process*. In brief, a stochastic process is called a *continuous Markov process* if it satisfies the Markov condition: For all  $t \geq 0, s \geq 0, \mathbb{P}[X(s+t) = j | X(s) = k \wedge X(u) : 0 \leq u < s] =$

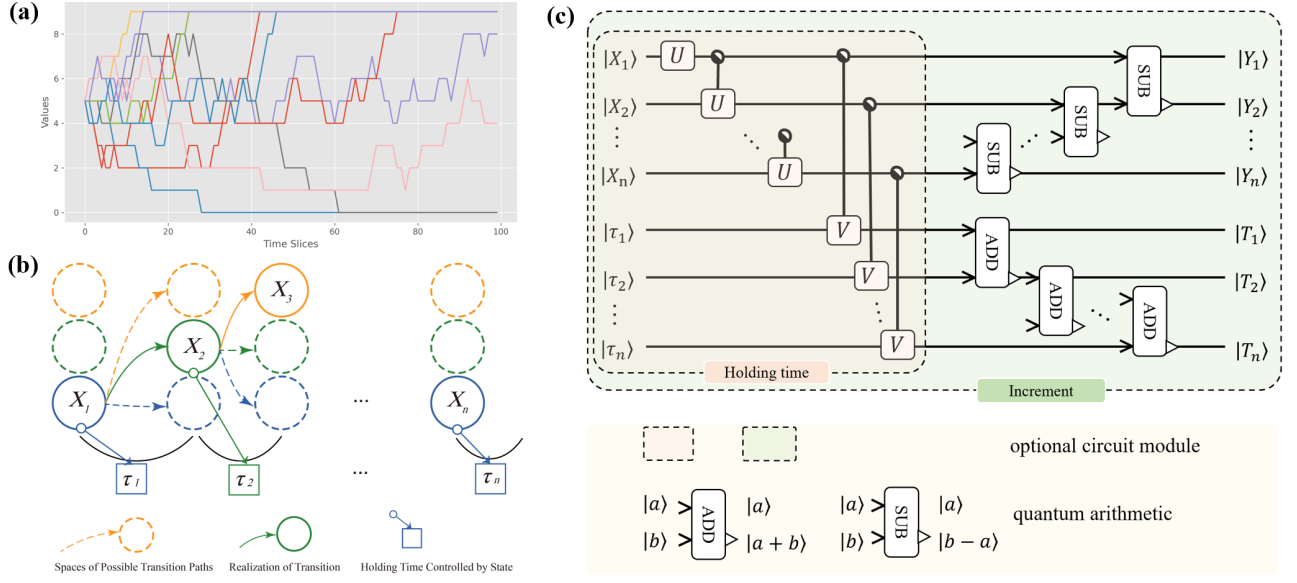


**FIG. 5. Prepare a Continuous Markov Process.** In this figure, the preparation of a continuous Markov Process is given: **(a)** 10 simulated *continuous Markov process* paths of 100 steps: The transition rates from  $|n\rangle$  to  $|n-1\rangle$  and  $|n+1\rangle$  are both 0.05, and the state  $|0\rangle$  and  $|10\rangle$  are absorbing states. Since the possibility of staying in the current state is  $p = 0.9$ , the continuous Markov process tends to be in-variant for a long holding time, and thus it can be compressed a lot via our encoding method. **(b)** The *continuous Markov process* is embedded via both holding time representation and increment representation. Due to  $\mathcal{ML}(X) = 1$ , each piece's state space  $X_j$  is controlled by the previous one  $X_{j-1}$  while the holding time  $\tau_j$  is determined by the current state  $X_j$  through an exponential distribution. **(c)** The preparation procedure of a *continuous Markov process* is shown. The embedded discrete Markov process  $X_j$  is prepared by a sequence of  $U$  and controlled- $U$  operators, while the holding time  $\tau_j$  is then determined by  $X_j$  and prepared by controlled- $V$  operators. The increment representation is then prepared by an alternative sequence of adder and subtractor subcircuits in the box.

$\mathbb{P}[X(s+t) = j | X(s) = k]$ , where  $j, k \in \mathcal{S}$ . Intuitively speaking, given the present state  $X(s)$ , the future  $\{X(s+t) : t \geq 0\}$  is independent of the past history  $\{X(u) : 0 \leq u < s\}$ , and the memory length of a *continuous Markov process* is  $\mathcal{ML}(X_t) = 1$  (shown in FIG. 5 **(a)** and **(b)**). A *continuous Markov process* can be efficiently prepared mainly for two reasons: the holding time  $\tau_j$  only depends on the current state  $X_j$ , while the state sequence  $\{X_j\}$  is independent from  $\{X_{j'} : 1 \leq j' < j-1\}$ . As a result, the *continuous Markov process* can be embedded into an independent discrete Markov chain depicting the transition probability, together with a sequence of controlled exponential distributions carrying the holding time information (as illustrated in FIG. 5 **(c)**). More precisely, we have the following result:

**Theorem 5. (Continuous Markov Process' Preparation)** *Supposing a stochastic process  $\{X(t) : t \geq 0\}$  with discrete state space  $\mathcal{S} \subseteq \mathbb{Z}$  to be a continuous-time Markov chain. Then it can be prepared on  $n \lceil \log(-\frac{S}{\lambda_{\min}} \ln \epsilon) \rceil$  qubits via a quantum circuit consisting of  $O(nS \lceil S + \log(-\frac{\ln \epsilon}{\lambda_{\min}}) \rceil)$  gates and  $nS^2$  circuit depth, where  $S = |\mathcal{S}|$ ,  $\lambda_{\min}$  is the minimum of  $\lambda_j$ , and  $\epsilon$  is the truncation error bound for time. (see proof in Appendix B4)*

### C. Cox process

As further evidence illustrating the flexibility and generalizability of our encoding method, the Cox process, a useful framework for modeling prices of financial instruments in financial mathematics [36], can be efficiently prepared. It is one of the most significant distinctions between the Cox process and those processes discussed above that both the states and the evolution law vary randomly over time (as illustrated in FIG. 6 **(a)** and **(b)**). As a direct consequence, the preparation procedure and the corresponding circuit should be dynamic and flexible to characterize this doubly stochastic property (shown in FIG. 6 **(c)**). Precisely speaking, a Cox process is a generalization of the Poisson process where the intensity  $\lambda(t)$  itself is also a stochastic variable of some distribution  $\mathcal{F}$ . The preparation procedure can be divided into two steps: Firstly, the stochastic control sequence of  $\lambda_j$  is prepared by some  $F$  operator for the underlying distribution  $\mathcal{W}$ . And secondly, the holding time sequence  $\tau_j$  is prepared by parallel controlled- $V$  operators for the underlying exponential distribution. The operators of different exponential distributions can be implemented by a sequence of controlled rotation gates of different rotation angles. The increments  $Y_j$  are assumed to be I.I.D. and can be prepared through some  $G$  operators (normal choice of distributions can be found in the appendix, see FIG. 15(a))



and FIG. 15(c) for reference). In summary, we have the following result:

**Theorem 6. (Cox Process' Preparation)** Suppose that  $\{X(t) : t \geq 0\}$  is a Cox process with varying intensity variable  $\lambda(t)$ , and  $\lambda(t)$  follows an underlying statistics distribution  $\mathcal{F}$  that can be prepared on  $q_{\mathcal{F}}$  qubits with circuit depth  $d_{\mathcal{F}}$ . The increments  $Y_j$  follows an I.I.D. that can be prepared on  $q_{\mathcal{G}}$  qubits with circuit depth  $d_{\mathcal{G}}$ . Also it is supposed that the minimum value of  $\lambda(t)$  is  $\lambda_{\min}$  and the error bound is  $\epsilon$ , then it can be efficiently prepared on  $O(n(q_{\mathcal{F}} + q_{\mathcal{G}} - \frac{\ln \epsilon}{|\lambda_{\min}|}))$  qubits with circuit depth  $O(\max\{q_{\mathcal{G}}, q_{\mathcal{F}} + 2^{d_{\mathcal{F}}}\} + nq_{\mathcal{G}})$  (holding time representation) or  $O(\max\{q_{\mathcal{G}}, q_{\mathcal{F}} + 2^{d_{\mathcal{F}}}\} - \frac{n \ln \epsilon}{\lambda_{\min}})$  (increment representation). (see proof in Appendix B5)

As the details of the QCTSP preparation procedure have been given above, the results are summarized in table II. From a high-level view, the computation and storage resource of the preparation procedure is totally determined by the time length  $T$  and the memory length  $\mathcal{ML}(X)$  of the underlying QCTSP  $X(t)$ . By our compressed encoding method and the corresponding preparation procedure, the number of copies of the state space is reduced from  $O(T) = O(n\tau_{avg})$  of the uniform sampling method to  $O(n \ln \tau_{avg})$  of the QCTSP method, leading an exponential reduction of qubit number on the parameter  $\tau_{avg}$ . By the encoding method and the observation on the holding time of the memory-less QCTSP, the circuit depths can be optimized from  $O(T \ln nS) = O(n\tau_{avg} \ln(nS\tau_{avg}))$  of the uniform sampling method to  $O(n \ln(nS))$  of the QCTSP method, also making an exponential reduction of qubit number on the parameter  $\tau_{avg}$ .

#### IV. INFORMATION EXTRACTION

Besides the state preparation problem, another challenge of QCTSP is to decode the compressed process and rebuild the information of interest. To extract desired information from QCTSP, instead of the discrete summation  $\mathbb{E}[f(S_n)] = \sum_{\mathbf{j} \in K^n} f(\text{sum}\{\mathbf{x}(\mathbf{j})\})\mathbb{P}[\mathbf{X} = \mathbf{x}(\mathbf{j})]$  as studied in [32], one needs to evaluate its continuous counterpart, i.e., the integral of random variable  $X$  on time  $t$ .

**Weightless Integral.** More specifically, the expectation value of an integrable function  $f : \mathbb{R} \rightarrow \mathbb{R}$  of the random variable

$$I(X, T) = \int_{t=0}^T X(t) dt \quad (6)$$

can be efficiently evaluated via a framework developed as follows: First of all, the integral can be divided into vertical boxes (as shown in FIG. 7 (a)) as a Riemann

summation

$$I(X, T) = \int_{t=0}^T X(t) dt = \sum_{j=0}^n X_j \tau_j.$$

Secondly, the area  $Z_j$  of each box is translated into multiplication on the holding time representation encoding variables  $X_j$  and  $\tau_j$ . Benefiting from the encoding method, this expression is quite simple (as illustrated in FIG. 7 (c)). Thirdly, the expected value of the integrable function  $f(\sum_{j=0}^n X_j \tau_j)$  can be evaluated through a Fourier approximation  $f_{P,L}(x) = \sum_{l=-L}^L c_l e^{i \frac{2\pi l}{p} x}$  as a  $P$ -periodic function of order  $L$ :

$$\sum_{l=-L}^L c_l (\mathbb{E}[\cos(\frac{2\pi l}{p}(\sum_{j=1}^n Z_j))] + i\mathbb{E}[\sin(\frac{2\pi l}{p}(\sum_{j=1}^n Z_j))]).$$

Each term  $\mathbb{E}[\cos(\frac{2\pi l}{p}(\sum_{j=0}^n Z_j))]$  and  $\mathbb{E}[\sin(\frac{2\pi l}{p}(\sum_{j=0}^n Z_j))]$  can be evaluated via rotation gates on the target qubit controlled by  $Z_j$  followed by a standard amplitude estimation algorithm. Leaving the detailed proof in the appendix, one has:

**Theorem 7. (Evaluating  $I(t)$ )** Suppose that a QCTSP  $\{X(t) : t \geq 0\}$  is given via holding time representation with  $n$  steps,  $l_x, l_\tau$  qubits for each pair  $X_j, \tau_j$ , and  $\mathcal{P}$  circuit depth. Also, one has that  $f_{P,L}(x)$  is the  $P$ -periodic  $L$ -order Fourier approximation of the desired integrable function of the random variable  $f : \mathbb{R} \rightarrow \mathbb{R}$ . Then given the error  $\epsilon$ , the expectation value of  $f(I(X, T)) = f(\int_{t=0}^T X(t) dt)$  can be efficiently evaluated within  $O(\mathcal{P} + nl_x l_\tau)$  circuit depth and  $O(\frac{LP}{\epsilon}(\mathcal{P} + nl_x l_\tau))$  time complexity. (see proof in Appendix C1)

**Weighted Integral.** Moreover, this framework applies to the more complicated and generalized situations where the time structure is considered and thus has no discrete correspondence. By introducing a time-dependent function  $g(t)$ , we can evaluate the expectation value of an integrable function  $f : \mathbb{R} \rightarrow \mathbb{R}$  of the random variable

$$J(X, T) = \int_{t=0}^T g(t)X(t) dt. \quad (7)$$

Since the time structure  $g(t)$  is considered, the integral is divided into horizontal directed boxes (as shown in FIG. 7 (b)):

$$J(X, T) = \sum_{j'=1}^n Y_{j'} (\sum_{j=j'}^n G_j) = \sum_{j=1}^n W_j.$$

Due to a trade-off on circuit depth and qubits number (see FIG. 7 (d) and FIG. 7 (e) for reference), this summation can be evaluated via either holding time representation or

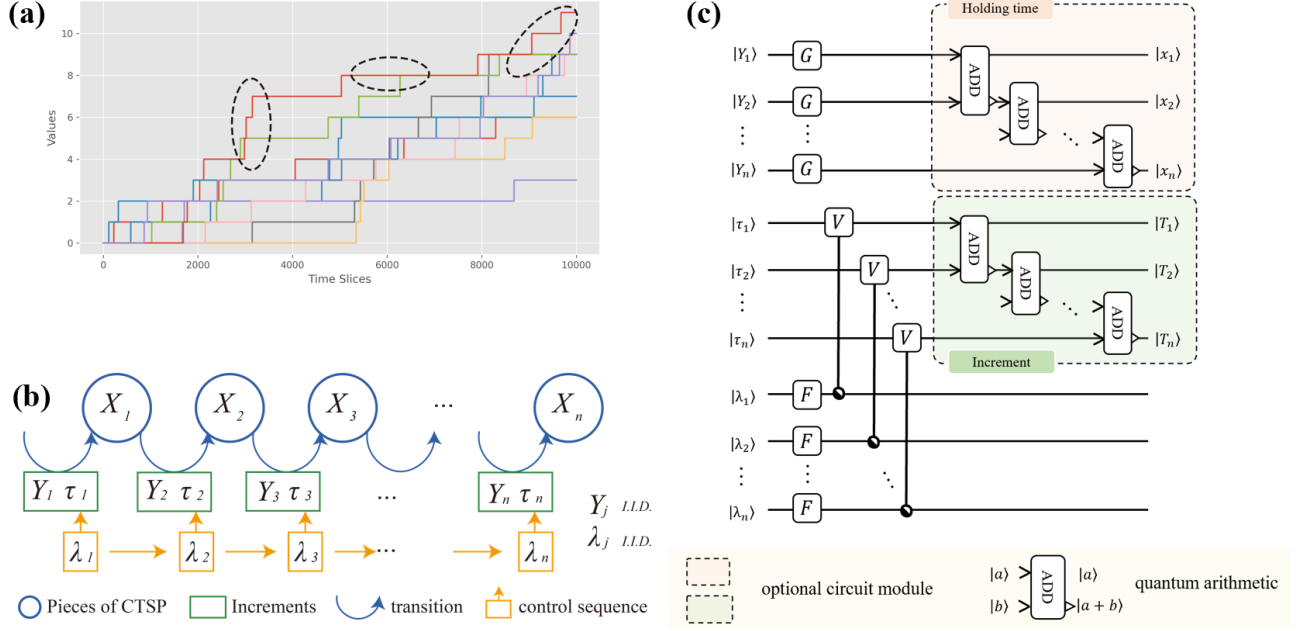


FIG. 6. **Prepare a Cox Process.** In this figure, the preparation of a continuous Markov Process is given: **(a)** 10 simulated Cox process paths of length 10 and 10000 steps: The varying intensity follows an exponential distribution with  $\lambda = 0.1$ , and the size of the discontinuous jump is assumed to be a constant 1. As circled in the picture, the intensity changes with time and the jump rate varies from high to low randomly. **(b)** A Cox Process is again embedded via holding time representation and increment representation encoding methods. The process is more complicated as the holding time  $Y_j$  of interest is controlled by another stochastic variable  $\lambda_j$  and the increment  $Y_j$  and the control variable  $\lambda_j$  are independent identical distribution variables, respectively. **(c)** The preparation of a Cox process is shown. Firstly, the stochastic control sequence  $\lambda_j$  is prepared by  $F$  operators, and then the holding time sequence  $\tau_j$  is prepared by parallel controlled- $V$  operators. The increments  $Y_j$  are I.I.D. and can be prepared through  $G$  operators. Alternative subcircuits of holding time and increment representations follow as shown in the two boxes.

increment representation. A similar Fourier approximation and amplitude estimation are employed to compute

$$\sum_{l=-L}^L c_l \left( \mathbb{E} \left[ \cos \left( \frac{2\pi l}{p} \left( \sum_{j=1}^n W_j \right) \right) \right] + i \mathbb{E} \left[ \sin \left( \frac{2\pi l}{p} \left( \sum_{j=1}^n W_j \right) \right) \right] \right),$$

and hence the following result is given:

**Theorem 8. (Evaluating  $J(t)$ )** *i) Suppose a QCTSP  $\{X(t) : t \geq 0\}$  of holding time representation given with  $n$  steps,  $l_x, l_\tau$  qubits for each pair  $X_j, \tau_j$ , and  $\mathcal{P}$  circuit depth.  $g(t)$  is a function whose integral can be efficiently prepared with  $\mathcal{F}$  circuit depth. Also, one has that  $f_{P,L}(x)$  is the  $P$ -periodic  $L$ -order Fourier approximation of the desired integrable function of the random variable  $f : \mathbb{R} \rightarrow \mathbb{R}$ . Then given the error  $\epsilon$ , the expectation value of  $f(J(X, T)) = f(\int_{t=0}^T g(t)X(t) dt)$  can be efficiently evaluated within  $\mathcal{P} + \mathcal{F} + nl_x l_\tau + n \max(l_x, l_\tau)$  circuit depth and  $O(\frac{LP}{\epsilon}(\mathcal{P} + \mathcal{F} + nl_x l_\tau + n \max(l_x, l_\tau)))$  time complexity.*

*ii) Suppose a QCTSP  $\{X(t) : t \geq 0\}$  of increment representation given with  $n$  steps,  $l_Y, l_T$  qubits for each pair  $Y_j, T_j$ , and  $\mathcal{P}$  circuit depth.  $g(t)$  is a function whose integral can be efficiently prepared with  $\mathcal{G}$  circuit depth. Also, one has that  $f_{P,L}(x)$  is the  $P$ -periodic  $L$ -order Fourier*

*approximation of the desired integrable function of the random variable  $f : \mathbb{R} \rightarrow \mathbb{R}$ . Then given the error  $\epsilon$ , the expectation value of  $f(J(X, T)) = f(\int_{t=0}^T g(t)X(t) dt)$  can be efficiently evaluated within  $O(\mathcal{P} + \mathcal{G} + nl_Y l_T)$  circuit depth and  $O(\frac{LP}{\epsilon}(\mathcal{P} + \mathcal{G} + nl_Y l_T))$  time complexity. (see proof in Appendix C2)*

Therefore our algorithms would enable the quantum Monte Carlo method to apply to path-dependent and continuous stochastic processes, including the time-weighted expectation  $\mathbb{E}[f(\frac{1}{T} \int_{t=0}^T tX(t) dt)]$  and the exponential decay time-weighted expectation  $\mathbb{E}[f(\int_{t=0}^T e^{-\alpha t} X(t) dt)]$  that are usually used in mathematical finance and quantitative trading.

**history-sensitive information.** Besides the global information defined on the whole path studied above, there is another category of history-sensitive problems that plays an essential role in statistics and finance, including the first-hitting time of Brownian motion, surviving time of ruin theory, and survival analysis, to name but a few. The most apparent difference of the first-hitting problem is that the path-dependent information needs to be extracted when knowing the whole history path. Thus it can not be derived directly by a quantum walk (as il-

lustrated in Fig. 8). Formally, a first-hitting problem can be regarded as evaluating the following

$$K(X, T, B) = \inf \{t : X(t) > B, T > t > 0\}. \quad (8)$$

The basic idea to evaluate Eq.(8) is to consider  $n$  flag qubits storing the comparison result of each piece in the sampling path. As a discontinuous jump representing extreme events or market hits always happens at the end of a piece, this method shall work much more precisely than the uniform sampling method. Formally speaking, supposing a given bound  $B$ , to derive the first hitting time, a bound information register and a flag register is introduced with  $O(\log B)$  and  $n$  qubits, respectively. For the  $j^{\text{th}}$  piece of QCTSP, the remained value is derived through a controlled subtraction whose control qubit is  $F_{j-1}$  and carry-out qubit is  $F_j$ . And a CNOT gate is implemented to flip the  $F_j$  qubit controlled by the  $F_{j-1}$  qubit. Two classes are distinguished for each piece: Before the first hit, the remaining bound is  $\sum_{j'=1}^{j-1} Y_{j'} \leq B$ , and the flag register is  $\underbrace{|11\dots 10\dots 0\rangle}_{j-1} \text{flag}$ . This first class

can be divided into two cases: If the hit does not happen at the  $j^{\text{th}}$  piece, the state of the carry-out qubit  $F_j$  after the subtraction remains  $|0\rangle$ , and then is flipped by the CNOT gate. Hence one has:

**case 1** ( $\sum_{j'=1}^{j-1} Y_{j'} \leq B$  and  $\sum_{j'=1}^j Y_{j'} < B$ ):

$$\begin{aligned} & |B - \sum_{j'=1}^{j-1} Y_{j'}\rangle_{\text{bound}} \underbrace{|11\dots 10\dots 0\rangle}_{j-1} \text{flag} \\ \xrightarrow{\text{controlled}} & |B - \sum_{j'=1}^j Y_{j'}\rangle_{\text{bound}} \underbrace{|11\dots 10\dots 0\rangle}_{j-1} \text{flag} \\ \xrightarrow{\text{subtractor}} & \\ \xrightarrow{\text{CNOT}} & |B - \sum_{j'=1}^j Y_{j'}\rangle_{\text{bound}} \underbrace{|11\dots 10\dots 0\rangle}_j \text{flag}. \end{aligned}$$

If the hit happens at the  $j^{\text{th}}$  piece, the state of the carry-out qubit  $F_j$  after the subtraction turns to be  $|1\rangle$ , and then is flipped by the CNOT gate. Hence one has:

**case 2** ( $\sum_{j'=1}^{j-1} Y_{j'} \leq B$  and  $\sum_{j'=1}^j Y_{j'} > B$ ):

$$\begin{aligned} & |B - \sum_{j'=1}^{j-1} Y_{j'}\rangle_{\text{bound}} \underbrace{|11\dots 10\dots 0\rangle}_{j-1} \text{flag} \\ \xrightarrow{\text{controlled}} & |B - \sum_{j'=1}^j Y_{j'}\rangle_{\text{bound}} \underbrace{|11\dots 10\dots 0\rangle}_j \text{flag} \\ \xrightarrow{\text{subtractor}} & \\ \xrightarrow{\text{CNOT}} & |B - \sum_{j'=1}^j Y_{j'}\rangle_{\text{bound}} \underbrace{|11\dots 10\dots 0\rangle}_{j-1} \text{flag} \end{aligned}$$

For the second class where the current piece is after the first hit  $\sum_{j'=1}^{j''} Y_{j'} > B$ , the flag register is  $\underbrace{|11\dots 10\dots 0\rangle}_{j''} \text{flag}$ , and the subtraction and CNOT gates will not be implemented, and thus the result is:

**case 3** ( $\sum_{j'=1}^{j''} Y_{j'} > B$  for some  $j'' < j$ ):

$$\begin{aligned} & |B - \sum_{j'=1}^{j''} Y_{j'}\rangle_{\text{bound}} \underbrace{|11\dots 10\dots 0\rangle}_{j''-1} \text{flag} \\ \xrightarrow{\text{controlled}} & |B - \sum_{j'=1}^{j''} Y_{j'}\rangle_{\text{bound}} \underbrace{|11\dots 10\dots 0\rangle}_{j''-1} \text{flag} \\ \xrightarrow{\text{subtractor}} & \\ \xrightarrow{\text{CNOT}} & |B - \sum_{j'=1}^{j''} Y_{j'}\rangle_{\text{bound}} \underbrace{|11\dots 10\dots 0\rangle}_{j''-1} \text{flag} \end{aligned}$$

Leaving the theoretical analysis as future work, examples of option pricing and ruin theory will be given in the next section as proof of principle.

## V. APPLICATION

In this section, two applications of QCTSP in different financial scenes are given to illustrate the wide range of applicability of QCTSP. In subsection **V A**, the first application is focused on the option pricing problem where the underlying stock price is no longer continuous Brownian motion and the original *Black-Scholes* formula fails. By simulation of QCTSP, option pricing is solved in a different way from previous works and is consistent with the more practical *Merton Jump Diffusion* formula. In subsection **V B**, the problem of computing the ruin probability under the *Collective Risk Model* is studied, introducing quantum computation into insurance mathematics.

### A. Option pricing in Merton Jump Diffusion Model

Since first being introduced into the field of financial engineering, CTSP has been proven to be a powerful tool for financial derivatives pricing [37, 38]. Among those financial derivatives, the European call option is one basic instrument that gives someone the right to buy an underlying stock  $S_T$  by a given knock price  $K$  at the fixed maturity time  $T$ . The famous *Black-Scholes* model is proposed to evaluate a European option [39], and the simulation for *Black-Scholes* type option pricing has been implemented on quantum computers [28–30, 32]. However, the assumption of a constant variance log-normal distribution in the original article [39] turns out to be less realistic as the empirical studies of discontinuous returns of stock are ignored. Hence the *Merton Jump Diffusion Model* was proposed to incorporate more realistic assumptions from Merton's work [40].

In the *Merton Jump Diffusion Model*, the stock price  $S_T$  is assumed to satisfy the following stochastic differ-

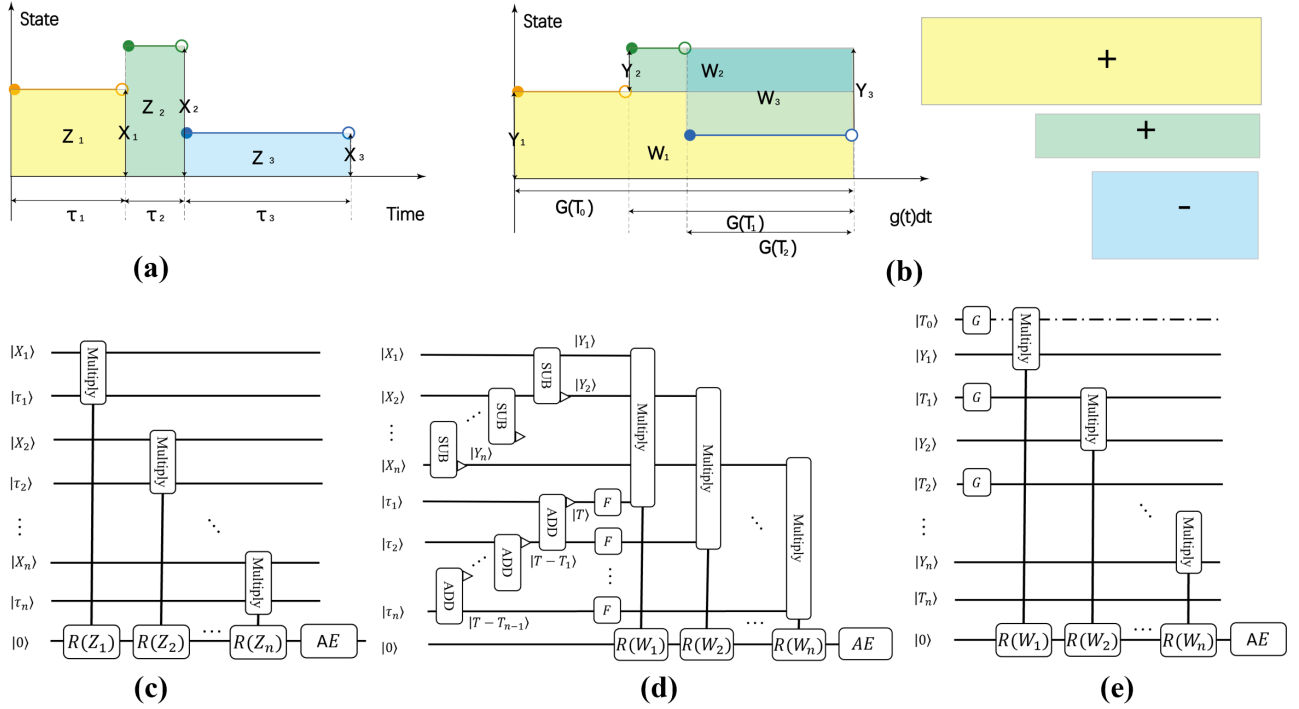


**FIG. 7. Information Extraction for Quantum Continuous Time Stochastic Process.** (a) The integral  $I(X, T) = \int_{t=0}^T X(t) dt$  is represented as a summation of the area of rectangles derived from vertical division  $I = \sum Z_j$ . (b) By a coordinate transformation  $t \rightarrow g(t)$ , the integral  $J(X, T) = \int_{t=0}^T g(t)X(t) dt$  can be represented as a summation of the directed area of rectangles derived from horizontal division  $J = \sum W_j$ : the yellow and green boxes both correspond to positive increments  $Y_{1,2}$  and area  $W_{1,2}$ , while the blue box corresponds to a negative increment  $Y_3$  and  $W_3$ . (c) The circuit for evaluating  $I(t)$  is shown. Supposing that  $X_j$  and  $\tau_j$  have been prepared as the input state,  $n$  quantum multipliers are introduced to evaluate  $Z_j = X_j\tau_j$ : Rotation operators controlled by  $Z_j$  are implemented on the target qubit, followed by a standard amplitude estimation subcircuit in the red box. (d) The circuit for evaluating  $J(t)$  of holding time representation is shown. Supposing that  $X_j$  and  $\tau_j$  have been prepared as the input state, then a sequence of subtractor operators is introduced to derive the increments  $Y_j$ , and another sequence of adder operators is introduced to evaluate the cumulative time from ending time  $T - T_{j-1} = \sum_{j'=j}^n \tau_{j'}$ . Hence  $\int_{T_{j-1}}^T g(t) dt = F(T - T_{j-1})$  can be evaluated through the integral operators  $F$ . Following that are the desired variables  $W_j = Y_j F(T - T_{j-1})$  by quantum multiplier operators: Rotation operators controlled by  $W_j$  are implemented on the target qubit, followed by a standard amplitude estimation subcircuit in the red box. (e) The circuit for evaluating  $J(t)$  of increment representation is shown. Supposing that  $Y_j$  and  $T_j$  have been prepared as the input state, one more qubit is introduced to denote the beginning time  $T_0$ , followed by unitary operators  $G$  act on  $T_j$  to derive  $G(T_{j-1})$ . Then a sequence of multiplier operators are implemented to compute the desired product  $W_j = Y_j G(T_{j-1})$ : Rotation operators controlled by  $W_j$  are implemented on the target qubit, followed by a standard amplitude estimation subcircuit in the red box. The circuit's depth is less than in subfigure (d) as a consequence of increment representation's advantage on integral calculation.

ential equation:

$$\begin{aligned} \ln S_T &= \ln S_0 + \int_{t=0}^T \left( r - \frac{\sigma^2}{2} - \lambda \left( m + \frac{v^2}{2} \right) \right) dt \\ &+ \int_{t=0}^T \sigma dW(t) \\ &+ \sum_{j=1}^{Poi(T)} (J_j - 1), \end{aligned} \quad (9)$$

where  $S_0$  is the current stock price,  $T$  is the maturity time in years,  $r$  is the annual risk-less interest rate,  $\sigma$  is the annual volatility,  $dW(t)$  is the Weiner process,  $Poi(T)$  is the *Poisson point process*, and  $J_j$  is the  $j^{th}$  discontinuous jump follows a log-normally distribution. The last

term on the right hand side represents the discontinuous price movements caused by such as acquisitions, mergers, corporate scandals, and fat-finger errors. Merton derives a closed form solution  $MJD(S, K, T, r, \sigma, m, v, \lambda)$  to Eq.(9) as an infinite summation of *Black-Scholes* formula  $BS(S, K, T, r_j, \sigma_j)$  conditional on the number of the jumps and the underlying distributions of each jump:

$$MJD(S, K, T, r, \sigma, m, v, \lambda) = \sum_{j=0}^{\infty} BS(S, K, T, r_j, \sigma_j), \quad (10)$$

where  $m$  is the mean of the jump size,  $v$  is the volatility of the jump size,  $\lambda$  is the intensity of the underlying *Poisson point process*, and  $r_j = r - \lambda(m - 1) + \frac{j \ln m}{T}$  and

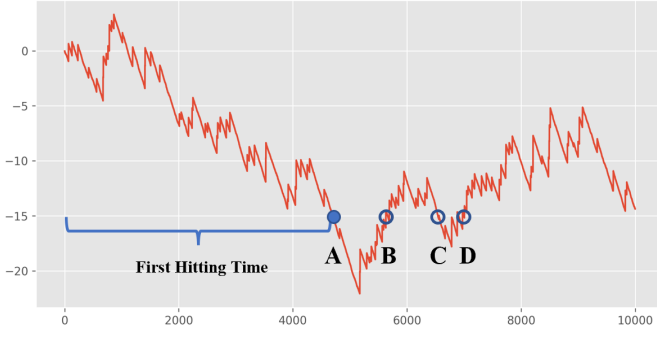


FIG. 8. As shown in this figure, the point **A** represents the first hitting event with the desired first hitting time, while the points **B**, **C**, **D** should not be captured. This information is determined by the knowledge of the whole past path, hence being *history-sensitive*, and can not be extracted by a quantum walk.

$\sigma_j = \sqrt{\sigma^2 + j \frac{v^2}{T}}$  are the corresponding interest rate and volatility, respectively. Despite being in line with empirical studies of market returns, the formula Eq. (10) takes the form of an infinite summation, and thus an alternative numerical method of Monte Carlo can be employed to compute the desired option price. Instead of a Brownian motion in the *Black-Scholes* model, one has to simulate, in the *Merton Jump Diffusion Model*, the more complicated case of a Lévy process where our method can be applied to make a quadratic speed-up against the classical Monte Carlo simulation. More precisely, for a European type call option given the underlying stock price  $S_T$ , its price can be defined as:

$$\begin{aligned} \text{price} &= \max\{S_0 e^{D+B_T + \sum_{j=1}^{Poi(T)} J_j} - K, 0\} \\ &= S_0 e^{\max\{D+B_T + \sum_{j=1}^{Poi(T)} J_j, \ln \frac{K}{S_0}\}} - K, \end{aligned} \quad (11)$$

where  $D = (r - \frac{\sigma^2}{2} - \lambda(m + \frac{v^2}{2}))T$  is the adjusted drift term on the purpose of risk neutral preferences,  $B_T$  represents the Brownian motion term and follows a normal distribution  $N(0, \sigma\sqrt{T})$ , and  $J_j$  represents the  $j^{\text{th}}$  discontinuous jump and follows a normal distribution  $N(m, v)$ .

This Lévy process can be efficiently prepared as mentioned in subsection III A, and then the valuation procedure is implemented via the method given in section IV. More specifically, as illustrated in Fig. 9, the quantum circuit consists of six quantum registers: the maturity time register  $|T\rangle$ , the holding time register  $|\tau_j\rangle$ , the flag register  $|F_j\rangle$ , the jump size register  $|B_j\rangle$ , the Brownian motion size register  $|G\rangle$ , and the target qubit  $|Target\rangle$ . The holding time  $\tau_j$  can be prepared via parallel exponential distribution subcircuits  $\mathcal{J} = Exp(\lambda T)$ , and the jump size  $B_j$  can be prepared via parallel normal distribution subcircuits  $\mathcal{B} = Norm(m, v)$ . The drift term together with the geometric Brownian motion is prepared on  $|G\rangle$  via a normal distribution subcircuit  $D + \mathcal{B}' = Norm((r - \frac{\sigma^2}{2} - \lambda(m + \frac{v^2}{2}))T, \sigma\sqrt{T})$ . Subtractor and controlled-subtractors, together with X gate

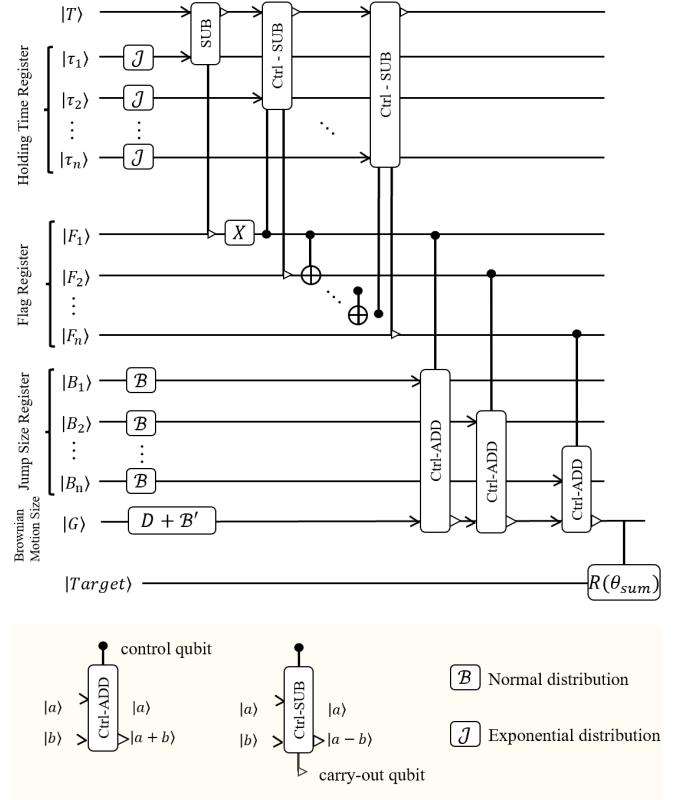


FIG. 9. **QCTSP Circuit of the Simulation of Merton Jump Diffusion Model.** In this figure, the circuit of the simulation of the European call option price in *Merton Jump Diffusion Model* is presented. The holding time  $\tau_j$  is prepared via parallel subcircuits  $\mathcal{J} = Exp(\lambda T)$ , and the jump size  $B_j$  is prepared via subcircuits  $\mathcal{B} = Norm(m, v)$ . The drift term, together with the geometric Brownian motion, is prepared on  $|G\rangle$  via the subcircuit  $D + \mathcal{B}' = Norm((r - \frac{\sigma^2}{2} - \lambda(m + \frac{v^2}{2}))T, \sigma\sqrt{T})$ . Subtractor and controlled-subtractors, together with X gate and CNOT gates, are implemented to justify the number of jumps with output on the flag register  $|F_j\rangle$ . Adders controlled by the flag registers are employed to derive the final value of the stock price, followed by a rotation gate on the target qubit controlled by the signed summation on register  $|\theta_{sum}\rangle$ .

and CNOT gates, are implemented to justify the number of jumps that will be considered, and the result is output on the flag register  $|F_j\rangle$ . Adders controlled by the corresponding flag registers are employed to derive the final value of the stock price. A rotation gate is then implemented on the target qubit, controlled by the signed summation on register  $|\theta_{sum}\rangle$ . Then the final value of the option price can be evaluated via measurement or an amplitude estimation.

The corresponding quantum simulation result can be found in Fig. 10 and Fig. 11. In Fig. 10, the underlying stock price is given with  $S_0 = 100$ ,  $K = 100$ ,  $r = 0.1$ ,  $\sigma = 0.02$ ,  $T = 1$ , and  $\Delta t = \frac{1}{30}$ , and the range of  $m$  and  $v$  are 0, 0.1, 0.2, 0.3, 0.4 and 0, 0.05, 0.15, 0.2, 0.25, respectively. Due to the restriction on the qubit number,



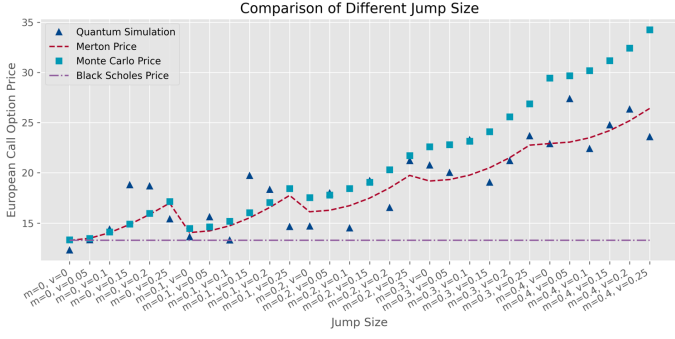


FIG. 10. **Comparison of QCTSP Simulation of European Call Option Price in Merton Jump Diffusion Model with Different Jump Size.** The simulation of European call option price in *Merton Jump Diffusion Model* is presented in this figure. The underlying stock price is given with  $S_0 = 100$ ,  $K = 100$ ,  $r = 0.1$ ,  $\sigma = 0.02$ ,  $T = 1$ , and  $\Delta t = \frac{1}{30}$ , and the range of  $m$  and  $v$  are 0, 0.1, 0.2, 0.3, 0.4 and 0, 0.05, 0.1, 0.15, 0.2, 0.25, respectively. As shown in the figure, the simulated prices are consistent with the Merton formula Eq.(10), and the value is away from the *Black Scholes* formula as the jump size tends to be large.

the simulation is divided into two steps: 100 groups of random rotation angles corresponding to the Brownian motion size. The jump sizes are generated by a classical random generator and then implemented on the target qubit. 1024 shots of QCTSP simulated paths are repeated for each group. As shown in Fig. 10, the larger the jump size (characterized by  $m$  and  $v$ ) is, the farther the *Merton Jump Diffusion* value is away from the original *Black-Scholes* price as a consequence of the discontinuous jumps. Moreover, the QCTSP simulation result is consistent with the 40 terms truncated *Merton Jump Diffusion* formula (Eq. (10)) as well as the classical Monte Carlo simulation, characterizing the property of Lévy discontinuous jump path well. The robustness of the QCTSP method is illustrated in Fig. 11, where different annual interest rates  $r = 0.05, 0.1, 0.15$  are given in the three subfigures with varying jump sizes. As shown in this figure, the quantum simulation results are consistent with the Merton Formula for a wide range of different parameters.

### B. Ruin probability in Collective Risk Model

Since being a fundamental means to model the stochastic world, there is no surprise that the QCTSP framework developed in this work has great potential power applied to various fields, especially ruin theory. The ruin theory plays a central role in insurance mathematics, high-frequency trading's market micro-structure theory, and option pricing [41–44]. In ruin theory, the risk of an insurance company is assumed to be caused by random claims arriving at time  $T_j = \sum_{j'=1}^j \tau_{j'}$ , wherein the  $j^{\text{th}}$  claim size  $\xi_j$  and inter-claim time  $\tau_j$  are both assumed

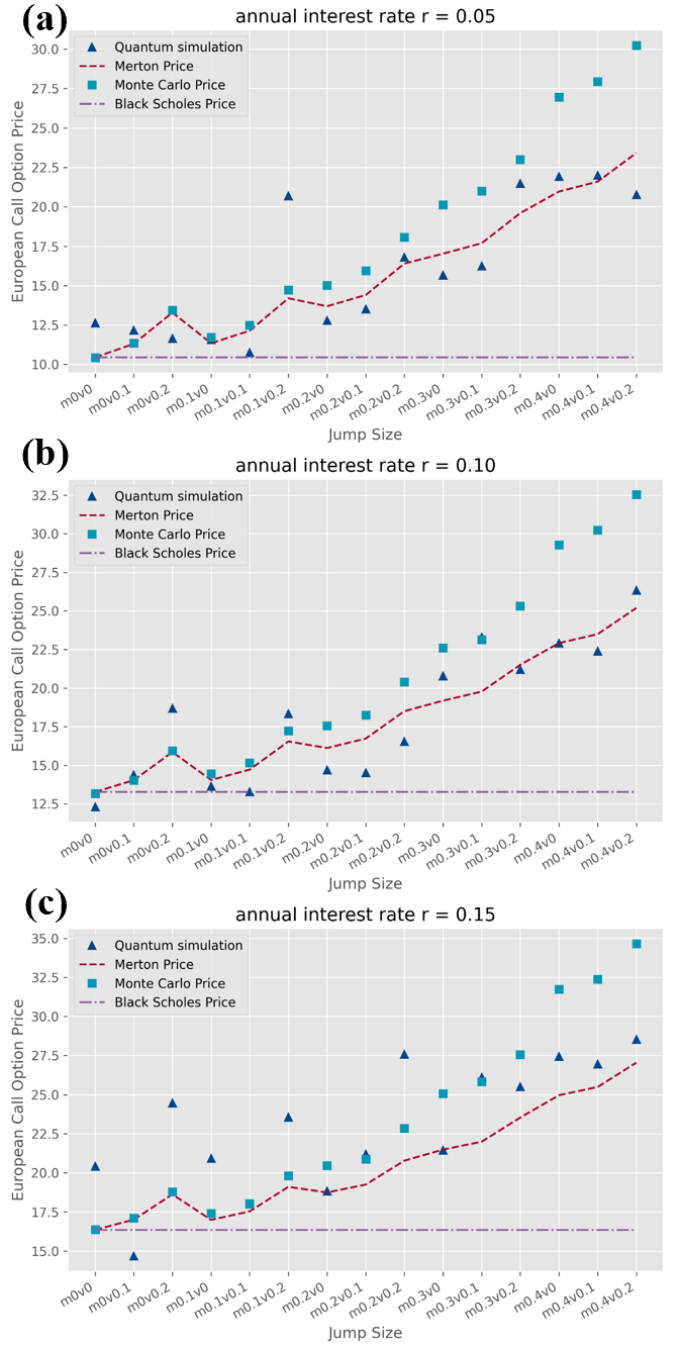


FIG. 11. **Comparison of QCTSP Simulation of European Call Option Price in Merton Jump Diffusion Model with Different Annual Interest.** The simulation of European call option price in *Merton Jump Diffusion Model* is presented in this figure. The underlying stock prices of annual interest rate  $r = 0.05, 0.1, 0.15$  are given with  $S_0 = 100$ ,  $K = 100$ ,  $\sigma = 0.02$ ,  $T = 1$ , and  $\Delta t = \frac{1}{30}$ , and the range of  $m$  and  $v$  are 0, 0.1, 0.2, 0.3, 0.4 and 0, 0.1, 0.2, respectively. As shown in the figure, the simulation results are consistent with the Merton formula Eq.(10) while the interest rate, the average jump size, and the volatility of jump size vary, showing robustness with wide ranges of parameters.

to follow some independent and identically distributions. Hence the aggregate asset of the insurance company is a continuous time stochastic process

$$X(t) = u + ct - \sum_{j=1}^{Poi(t)} \xi_j, \quad (12)$$

where the initial surplus is  $X(0) = u$ , and the premiums are received at a constant rate  $c$ . In the *Collective Risk Model*, also known as the Cramér Lundberg model, the claim number process  $Poi(t)$  is assumed to be a Poisson process with intensity  $\lambda$ , and the underlying distribution of  $\tau_j$  is an exponential distribution. In the Sparre Andersen model,  $Poi(t)$  can be extended to a renewal process with the arbitrary underlying distribution. Despite the detailed differences between them, both of the two stochastic processes  $X(t)$  in these models are Lévy processes with drift term  $ct$ , and hence can be prepared easily via our method.

$$Y(t) = u + ct - X(t) = \sum_{j=1}^{Poi(t)} \xi_j \quad (13)$$

To go one step further, one has a great variety of ruin-related quantities fall into the category of the expected discounted penalty function, also known as the time value of ruin. And those can be easily derived through a quantum MC modified by us. More precisely, following the notation of Gerber and Shiu [41], the time value of ruin is defined as

$$\phi(u) = \mathbb{E}^{X_t} [e^{-\delta\tau} w(X(\tau-), X(\tau)) \mathbb{I}_{\tau < \infty} | X(0) = u], \quad (14)$$

where  $\tau(u) = \inf \{t : U(t) < 0 | U(0) = u\}$  denotes the time of ruin, and  $X(\tau-) = u + c\tau - \sum_{j=1}^{N(\tau)-1} X_j$  and  $X(\tau) = u + c\tau - \sum_{j=1}^{N(\tau)} X_j$  are the surplus prior to ruin and the deficit at ruin, respectively. The expectation is taken over the probability distribution of the ruin samples, taking an interest discounting factor  $e^{-\delta\tau}$  into consideration. The ultimate ruin probability  $\psi(u) = \mathbb{P}[X(\tau) < 0 | X(0) = u, \tau < \infty]$  is exactly a special case of Eq.(14) given  $\delta = 0$  and  $w(x, y) = 1$ . Since ruin always happens after a claim,

$$\begin{aligned} \psi(u) &= \mathbb{P}[X(\tau) < 0 | X(0) = u, \tau < \infty] \\ &= \mathbb{E}^{X_t} [\mathbb{I}_{\tau < \infty} | X(0) = u] \\ &= \mathbb{E}^{X_t} [\mathbb{I}_{u + \sum_{j=1}^n (\tau_j - \xi_j) < 0} | n < \infty] \\ &= \mathbb{E}^{Y_t} [\mathbb{I}_{Y(t) < u + ct}], \end{aligned}$$

where the indicator function  $\mathbb{I}_{Y(t) < u + ct}$  can be easily derived through a sequence of controlled adder and modified subtractor on the prepared states. The detailed construction of circuits and corresponding simulation result are given in Fig. 12 and Fig. 13.

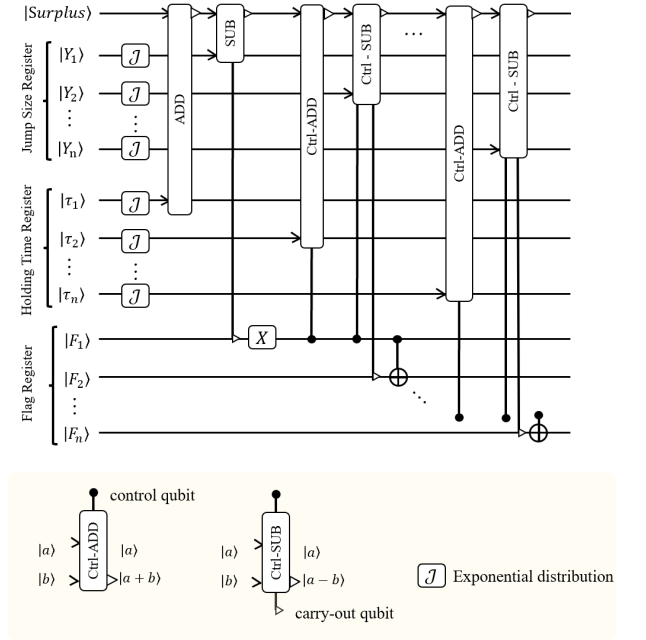


FIG. 12. **Quantum Circuit of Computing Ruin Probability.** The ultimate probability of the *Collective Risk Model* is simulated via this quantum circuit. The receiving rate is assumed to be 1 so that the premium can be summed directly, removing the qubits requirement and the circuit depth from function  $cT$ . For each piece of QCTSP, an adder is followed by a controlled-subtractor whose carry-out qubit is on the flag qubit together with a controlled flip, as discussed in subsection IV.

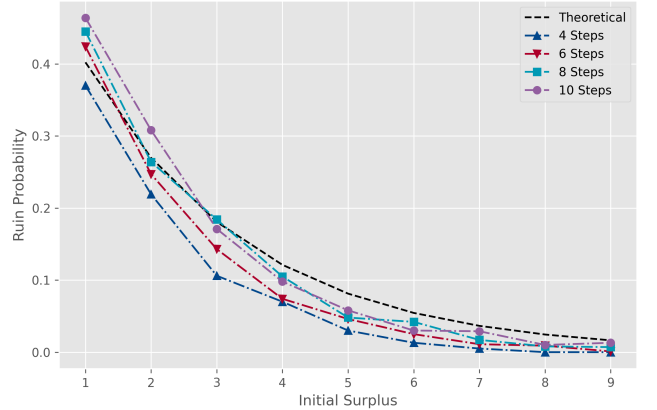


FIG. 13. **Simulation of ultimate ruin probability.** The ultimate probability of the *Collective Risk Model* is simulated for varying initial surplus with sample paths of different lengths. The intensities of inter-claim time and claim size are  $\lambda_t = 0.6$ , and  $\lambda_\xi = 1$ , respectively. The sample precision is  $\epsilon = 0.001$ , and the premiums' receiving rate is  $c = 1$ . The shot number is set to be 1000 for each simulation point. As shown in the figure, the simulated ruin probabilities of varying surpluses fit the theoretical benchmark well. And the distance from the theoretical curve tends to be smaller as the length of the sample paths grows.

TABLE II. **Comparison of QCTSP and Uniform Sampling** In this table, most often-used CTSP's preparation procedure is summarized: the memory length, qubit number and circuit depth of each CTSP type, which have been given in section III and proved in Appendix B, are listed in the second, third, and fifth columns, respectively.

QCTSP Type	$\mathcal{ML}$	Qubit Number		Circuit Depth	
		QCTSP (our work)	Uniform Sampling	QCTSP (our work)	Uniform Sampling
Poisson point process	0	$n \lceil \log(-\frac{n \ln \epsilon}{\lambda}) \rceil$	$\frac{-n \ln \epsilon}{\lambda} \lceil \log(-\frac{n \ln \epsilon}{\lambda}) \rceil$	$\lceil \log n \rceil$	$\lceil \log(-\frac{n \ln \epsilon}{\lambda}) \rceil$
compound Poisson process	0	$n \lceil \log(-\frac{-nS \ln \epsilon}{\lambda}) \rceil$	$\frac{-n \ln \epsilon}{\lambda} \lceil \log(-\frac{-nS \ln \epsilon}{\lambda}) \rceil$	$S + n \lceil \log(nS) \rceil$	$S + \frac{-n \ln \epsilon}{\lambda} \lceil \log(-\frac{-nS \ln \epsilon}{\lambda}) \rceil$
Lévy process	0	$n \log(nS')$	$T \log S$	$S' + n \lceil \log(nS') \rceil$	$S + T \log(TS)$
continuous Markov process	1	$n \lceil \log(-\frac{S \ln \epsilon}{\lambda_{min}}) \rceil$	$-\frac{n \ln \epsilon}{\lambda_{min}} \lceil \log(-\frac{S \ln \epsilon}{\lambda_{min}}) \rceil$	$nS^2$	$-\frac{n \ln \epsilon}{\lambda_{min}} S^2$
$k$ -order Markov process	$k$	$n \lceil \log(-\frac{S \ln \epsilon}{\lambda_{min}}) \rceil$	$-\frac{n \ln \epsilon}{\lambda_{min}} \lceil \log(-\frac{S \ln \epsilon}{\lambda_{min}}) \rceil$	$nS^{k+1}$	$-\frac{n \ln \epsilon}{\lambda_{min}} S^{k+1}$
Cox process	0	$n(q_{\mathcal{F}} + q_{\mathcal{G}} - \frac{\ln \epsilon}{ \lambda _{min}})$	$-\frac{n \ln \epsilon}{ \lambda _{min}} (q_{\mathcal{F}} + q_{\mathcal{G}})$	$\max\{q_{\mathcal{G}}, q_{\mathcal{F}} + 2^{d_{\mathcal{F}}}\} + nq_{\mathcal{G}}$	$\max\{q_{\mathcal{G}}, q_{\mathcal{F}} + 2^{d_{\mathcal{F}}}\} - \frac{nq_{\mathcal{G}} \ln \epsilon}{ \lambda _{min}}$
general CTSP	$n$	$n \log \frac{ST}{n}$	$T \log S$	$(\frac{ST}{n})^n$	$S^T$

## VI. DISCUSSION

In our work, the efficient state preparation and quantum-enhanced analysis of continuous time stochastic process are studied. The whole procedure for the QCTSP preparation is established: The state can be prepared to be more sensitive to discontinuous jumps modeling the extreme market emergencies. The qubit number and the circuit depth are both reduced exponentially on the key parameter of holding time. Also, a new Monte Carlo simulation method for QCTSP is proposed. The QCTSP admits a further quadratic speed-up against its classical counterpart CTSP as the mainstream instrument studying the continuous time stochastic world. The techniques for the extraction of *weighted integral* and *history-sensitive information*, essential for quantitative trading, time series analysis, and actuarial mathematics, are developed so that the requirement of extra  $n$  copies of random paths, and the implied restriction of I.I.D. condition can both be removed. Two applications on European option pricing under the *Merton Jump Diffusion Model* and the ruin probability evaluating in *Collective Risk Model* are given as proof of principle.

There are mainly four reasons why QCTSP is one of the proper candidates for practical application in the noisy intermediate-scale quantum eras. First of all, QCTSP has no input restriction and can be implemented without the assumption of quantum oracle and qRAM. What's more, it can be utilized within *quantum machine learning* and other quantum algorithms as a basic proce-

dure breaking through the input bottleneck. The second reason is that the QCTSP can be prepared parallel due to a communicative equivalence class decomposition of the sample space, resulting in a qubit number reduction. Thirdly, our QCTSP preparation method makes low requirements on the topological structure of the quantum processor: The connectivity requirement concerned with the memory length can be supposed to be quite low in many situations, and thus most qubits only need to be entangled with their neighborhood. Lastly, due to the fundamental and critical role CTSP plays in stochastic analysis, the QCTSP is believed to have huge potential for theoretical generalizability and applied flexibility.

In consideration of the conciseness and thematic focus, many interesting applications of QCTSP on different facets, such as high-frequency trading, actuarial, and option pricing, are left to be solved, too. Besides, more techniques on the efficient extraction of path-dependent information should be studied in the future.

## ACKNOWLEDGEMENT

This work was supported by the National Natural Science Foundation of China (Grants No. 12034018), and Innovation Program for Quantum Science and Technology No. 2021ZD0302300.

## Appendix A: Basic Circuits for Arithmetic and Distribution Preparation

Some basic arithmetic circuits and statistics distribution preparation circuits are given in this appendix.

### 1. Modified Quantum Subtractor

Although adder and subtractor circuits have been studied in many works (see [45] for reference), some modification is needed in our work as we wish to map  $|a\rangle|b\rangle$  to  $|a\rangle|a-b\rangle$ , i.e., store the result in the second register while leave the first register unchanged. The basic idea is as follows: since  $(a'+b)' = a-b$ , X gates are introduced to calculate the complement of  $a$  as  $|a'\rangle|b\rangle$ . Then a ripple-carry addition circuit is implemented to output the summation result on the first register  $|a'+b\rangle|b\rangle$ . Finally, another sequence of X gates are put on the first register  $|a-b\rangle|b\rangle$ .

### 2. Quantum Multiplier for Amplitude Estimation and Quantum Monte Carlo

In this subsection, a quantum multiplier for quantum estimation, and hence quantum Monte Carlo is given as follows:

**Lemma 9.** *Suppose that  $|a\rangle$  and  $|b\rangle$  are  $l_a$ -bit and  $l_b$ -bit strings, respectively, and  $|e^{iM\theta_0}\rangle$  is an analog-encoded qubit, then the multiplication of  $|a\rangle$  and  $|b\rangle$  can be added to  $|e^{iM\theta_0}\rangle$  as  $|a\rangle|b\rangle|e^{iM\theta_0}\rangle \rightarrow |a\rangle|b\rangle|e^{i(M+ab)\theta_0}\rangle$ , within  $l_a l_b$  controlled-rotation gates.*

*Proof.* The proof is directly: Given two bit strings  $|a\rangle = |x_{l_a} \dots x_2 x_1\rangle$  and  $|b\rangle = |y_{l_b} \dots y_2 y_1\rangle$ , their product can be computed as

$$\begin{aligned} ab &= \left( \sum_{i=1}^{l_a} x_i 2^{i-1} \right) \left( \sum_{j=1}^{l_b} y_j 2^{j-1} \right) \\ &= \sum_{i=1}^{l_a} \sum_{j=1}^{l_b} x_i y_j 2^{i+j-2}. \end{aligned}$$

Hence the term  $x_i y_j 2^{i+j-2}$  can be implemented by a rotation gate on the target qubit  $|e^{iM\theta_0}\rangle$  controlled by the  $i^{\text{th}}$  and  $j^{\text{th}}$  qubits of register  $|a\rangle$  and  $|b\rangle$ , where the rotation angle  $\theta_{i,j} = 2^{i+j-2}\theta_0$  is determined by the index  $i, j$  only. The final state is:

$$\begin{aligned} |e^{iM\theta_0}\rangle &\rightarrow \left| e^{i(M\theta_0 + \sum_{i=1}^{l_a} \sum_{j=1}^{l_b} x_i y_j 2^{i+j-2} \theta_0)} \right\rangle \\ &= \left| e^{i(M+ab)\theta_0} \right\rangle. \end{aligned}$$

If  $|a\rangle$  and  $|b\rangle$  are signed integers, the rotation gates of two different directions should be controlled by the two sign qubits as well. The total number of controlled rotation gates is  $l_a l_b$  as claimed.  $\square$

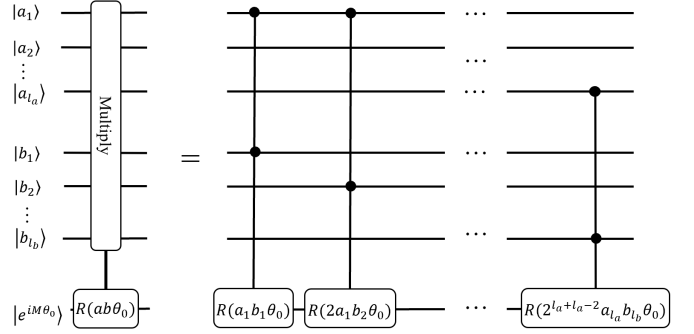


FIG. 14. **Modified Subtractor Circuit.** In this figure, a subtractor circuit of two 3-qubits integers that maps  $|a\rangle|b\rangle$  to  $|a-b\rangle|b\rangle$  is given. The basic idea is from [45] with some modification so that the result can be stored in the first register leaving the second register unchanged.

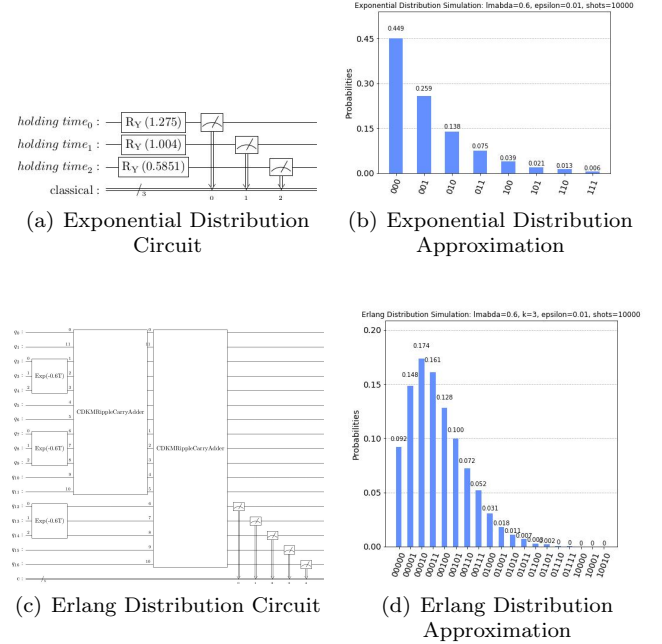


FIG. 15. Preparation of Exponential and Erlang Distribution

### 3. State preparation for Statistical Distributions

The exponential distribution is implemented by parallel rotation gates as illustrated in FIG. 15(a). Detailed computation of rotation angles is given in Appendix B 1. The Erlang distribution is a summation of several exponential distributions and hence can be prepared via copies of exponential distribution preparation subcircuits together with a sequence of adder operators as shown in FIG. 15(c). Corresponding simulation results are given in FIG. 15(b) and 15(d), respectively.

## Appendix B: Proofs for QCTSP State Preparation Problem

### 1. Proof of Theorem 1

*Proof.* By the definition of memory-less process, one has

$$\mathbb{P}[\tau_l > s] = \mathbb{P}[\tau_l > t + s | \tau_l > t] = \frac{\mathbb{P}[\tau_l > t + s]}{\mathbb{P}[\tau_l > t]},$$

and hence the c.d.f.  $f(t) = \mathbb{P}[\tau_l \leq t]$  satisfies:

$$1 - f(s) = \frac{1 - f(s+t)}{1 - f(t)}.$$

Differentiating with respect to  $t$  and setting  $t = 0$  leads to

$$\begin{aligned} -f'(s) &= \frac{-f'(s+t)}{1 - f(t)}, \\ -f'(0) &= \frac{-f'(t)}{1 - f(t)}. \end{aligned}$$

Noticing that  $-f'(0)$  is a constant, the integrals of the two sides turn to be

$$\begin{aligned} -f'(0)t &= \ln(1 - f(t)) + C \\ f(t) &= 1 - e^{-f'(0)t}, \end{aligned}$$

where the constant  $C$  is supposed to be exactly 1 to satisfy  $f(\infty) = 1$ . Thus the holding time  $\tau_l$  follows an exponential distribution  $\mathbb{P}[\tau_l \geq t] = e^{-\lambda_l t}$  with  $\lambda_l = f'(0)$  determined by  $X_l$ . As  $\epsilon$  is given, without loss of generality,  $T$  is supposed to be  $2^m$  with  $m = \lceil \log(-\frac{1}{\lambda_l} \ln \epsilon) \rceil$  so that

$$T = -\frac{1}{\lambda_l} \ln \tilde{\epsilon} \geq -\frac{1}{\lambda_l} \ln \epsilon, \quad (\text{B1})$$

where

$$\tilde{\epsilon} = e^{-\lambda_l T} < \epsilon \quad (\text{B2})$$

is a more strictly error bound which is easier to compute. On the truncated support set  $[0, T)$ , simple computation shows that

$$\bar{\mathbb{P}}[t \leq \tau < t+1] = \frac{\mathbb{P}[t \leq \tau < t+1]}{\mathbb{P}[0 \leq \tau < T]} = \frac{e^{-\lambda_l t} - e^{-\lambda_l(t+1)}}{1 - e^{-\lambda_l T}}. \quad (\text{B3})$$

Assuming that the preparation circuit consists of  $m = \log T$  qubits initialized to be  $|0\rangle$ , the  $j^{\text{th}}$  qubit is then aligned with the rotation gate  $R_Y(\theta_j)$  with  $\theta_j = \arctan \tilde{\epsilon}^{1/2^{j+1}} : 1 \leq j \leq m$ . A direct computation shows

that

$$\begin{aligned} & \bigotimes_{j=1}^m R_Y(\theta_j) |0\rangle \\ &= \bigotimes_{j=1}^m \left( \frac{1}{\sqrt{1 + \tilde{\epsilon}^{1/2^j}}} |0\rangle + \frac{\tilde{\epsilon}^{1/2^{j+1}}}{\sqrt{1 + \tilde{\epsilon}^{1/2^j}}} |1\rangle \right) \\ &= \bigotimes_{j=1}^m \left( \sum_{k_j=0}^1 \frac{\tilde{\epsilon}^{k_j/2^{j+1}}}{\sqrt{1 + \tilde{\epsilon}^{1/2^j}}} |k_j\rangle \right) \\ &= \sum_{k_1, k_2, \dots, k_m=0}^1 \frac{\tilde{\epsilon}^{\sum_{j=1}^m k_j/2^{j+1}}}{\prod_{j=1}^m \sqrt{1 + \tilde{\epsilon}^{1/2^j}}} |k_1 k_2 \dots k_m\rangle \\ &= \sum_{k_1, k_2, \dots, k_m=0}^1 \sqrt{\frac{1 - \tilde{\epsilon}^{1/2^m}}{1 - \tilde{\epsilon}}} \tilde{\epsilon}^{\sum_{j=1}^m \frac{k_j}{2^{j+1}}} |k_1 k_2 \dots k_m\rangle \\ &= \sum_{k_1, k_2, \dots, k_m=0}^1 \sqrt{\frac{\tilde{\epsilon}^{\sum_{j=1}^m \frac{k_j}{2^j}} - \tilde{\epsilon}^{\frac{1}{2^m} + \sum_{j=1}^m \frac{k_j}{2^j}}}{1 - \tilde{\epsilon}}} |k_1 k_2 \dots k_m\rangle \end{aligned} \quad (\text{B4})$$

$$= \sum_{t=0}^{T-1} \sqrt{\frac{\tilde{\epsilon}^{\frac{t}{T}} - \tilde{\epsilon}^{\frac{t+1}{T}}}{1 - \tilde{\epsilon}}} |t\rangle \quad (\text{B5})$$

$$= \sum_{t=0}^{T-1} \sqrt{\frac{e^{-\lambda_l t} - e^{-\lambda_l(t+1)}}{1 - e^{-\lambda_l T}}} |t\rangle \quad (\text{B6})$$

$$= \sum_{t=0}^{T-1} \sqrt{\bar{\mathbb{P}}[t \leq \tau < t+1]} |t\rangle \quad (\text{B7})$$

Here the binary number and the corresponding summation  $(k_1 k_2 \dots k_m)_2 = \sum_{j=1}^m k_j 2^{m-j}$  in Eq.(B4) are both substituted by the decimal number  $t$  varying from 0 to  $T = 2^m$  in Eq.(B5). Then Eq.(B6) and Eq.(B7) are derived by Eq.(B2) and Eq.(B3), respectively. Hence, with  $m = \lceil \log(-\frac{1}{\lambda_l} \ln \epsilon) \rceil$  qubits and the same number of rotation gates, the desired truncated state is successfully prepared((as illustrated in FIG. 15(a) and FIG. 15(b))).  $\square$

### 2. Proof of Theorem 2

*Proof.* Given a time interval  $T$ , it can be uniformly divided into  $n$  pieces  $[T_{j-1}, T_j)$  with  $T_j = \frac{j}{n}T$  ( $0 \leq j \leq n$ ) and  $\tau_j = \frac{T}{n} : 1 \leq j \leq n$ , and the corresponding discrete random variables are denoted by  $X_j = X(T_j)$ . Then the increments  $Y_1 = X_1$  and  $Y_j = X_j - X_{j-1} : 2 \leq j \leq n$  are independent and identically distributed random variables. The underlying distribution  $\mathcal{F}$  can be prepared by Grover's method  $|0\rangle_s \rightarrow |\mathcal{F}\rangle_j = \sum_{k=1}^S p_j(k) |k\rangle$ , where  $s = \log S$  is the number of qubits of the approximation  $\tilde{\mathcal{F}}_j$  and  $p_j(k)$  is the probability amplitude that the random variable  $X_j$  lies in the  $k^{\text{th}}$  interval of  $\tilde{\mathcal{F}}$  with  $\sum_{k=1}^S p_j^2(k) = 1$  (see [20] for reference). The circuit depth of the preparation of  $\tilde{\mathcal{F}}$  is at most  $s$  utilizing  $S$  control-rotation gates.



Then the increments sequence  $Y_j : 1 \leq j \leq n$  can be derived by repeating this procedure on  $n$  parallel subcircuits:  $|Y_1\rangle|Y_2\rangle\dots|Y_n\rangle = \bigotimes_{j=1}^n |\mathcal{F}\rangle_j$ . The desired path variables  $\{X_j = \sum_{j'=1}^j Y_{j'} : 1 \leq j \leq n\}$  are derived by a sequence of recursive add operators on these  $n$  registers as  $|Y_1\rangle|Y_2\rangle\dots|Y_n\rangle \rightarrow |Y_1\rangle|Y_1 \oplus Y_2\rangle|Y_3\rangle\dots|Y_n\rangle \rightarrow \dots \rightarrow |Y_1\rangle|Y_1 \oplus Y_2\rangle\dots|Y_1 \oplus Y_2 \oplus \dots \oplus Y_n\rangle = |X_1, X_2, \dots, X_n\rangle$  (See FIG. 4 (c)). Each add operator takes  $2 \log(nS) - 1$  Toffoli gates and  $5 \log(nS) - 3$  C-NOT gates. A simple computation shows that the circuit depth is  $S + (n - 1)(2 \log(nS) + 4) = O(S + n \log(nS))$  and the gate complexity is at most  $nS + (n - 1)(5 \log nS - 3 + 2 \log nS - 1) = O(n(S + \log(nS)))$  gates.  $\square$

### 3. Proof of Corollary 3 and Corollary 4

*Proof.* By definition of Poisson Point Process, the distinct increments  $Y_j : 1 \leq j \leq n$  are constant 1, and the  $X_j$  varies exactly from 1 to  $n$  so that the adder subcircuit introduced in Theorem 2 can be omitted. As a consequent, each  $X_j$  can be prepared parallel on at most  $\log n$  qubits via  $\log n$  rotation gates. And meanwhile the holding times  $\tau_j : 1 \leq j \leq n$  are assumed to follow an exponential distribution  $\mathcal{F}(\lambda)$ , and can thus be prepared parallel, by Theorem 1, on  $\frac{-\ln \epsilon}{\lambda}$  qubits via  $\frac{-\ln \epsilon}{\lambda}$  rotation gates with circuit depth 1. In summary, the qubit number, circuit depth and gate complexity are respectively  $n \log n + n \frac{-\ln \epsilon}{\lambda} = n \lceil \log(\frac{-n \ln \epsilon}{\lambda}) \rceil$ ,  $\max\{\lceil \log n \rceil, 1\} = \lceil \log n \rceil$ , and  $n \log \frac{-\ln \epsilon}{\lambda} + \sum_{j=1}^n \log j = O(n \lceil \log(\frac{-n \ln \epsilon}{\lambda}) \rceil)$ . As for the case of Compound Poisson Process, the only difference is the I.I.D. state space of jumps. Another  $n \lceil \log S \rceil$  qubits are introduced to record these jumps, and hence the qubits number turn to be  $n \lceil \log(\frac{-nS \ln \epsilon}{\lambda}) \rceil$ . Instead of copies of Hadamard gates in *Poisson point process*, a sequence of  $n - 1$  adder operators are needed, asking for  $(n - 1)(2 \lceil \log(nS) \rceil - 1)$  Toffoli gates and  $(n - 1)(5 \lceil \log(nS) \rceil - 3)$  C-NOT gates. Thus the total gate complexity is  $O(n \lceil \log(\frac{-nS \ln \epsilon}{\lambda}) \rceil)$ , and the circuit depth is  $S + n \lceil \log(nS) \rceil$ .  $\square$

### 4. Proof of Theorem 5

*Proof.* Assuming that the  $n$  pieces of the *continuous Markov process* are  $(X_j, \tau_j)$ , and the  $j^{\text{th}}$  transition time are  $T_j = \sum_{j'=1}^j \tau_{j'}$ , a direct computation shows that

$$\begin{aligned} & \mathbb{P}[X_{j+1} = k_{j+1} | \wedge_{j'=1}^j X_{j'} = k_{j'}] \\ &= \mathbb{P}[X(T_j) = k_{j+1} | \wedge_{j'=1}^j X(t) = k_{j'} : T_{j-1} \leq t < T_j] \\ &= \mathbb{P}[X(T_j) = k_{j+1} | X(t) = k_j : T_{j-1} \leq t < T_j] \\ &= \mathbb{P}[X_{j+1} = k_{j+1} | X_j = k_j]. \end{aligned} \tag{B8}$$

This reveals that  $X_{j+1}$  is totally determined by the previous state  $X_j$  with the transition probabilities  $P_{kl} =$

$P(X_{j+1} = k | X_j = l)$ , and thus the embedded sequence  $\{X_j : 1 \leq j \leq n\}$  is a discrete Markov chain as claimed above. By the Markov condition again, the holding time  $\tau_j$  satisfies

$$\mathbb{P}[\tau_j > t + s | \tau_j > t] = \mathbb{P}[\tau_j > s]. \tag{B9}$$

Noticing that Eq.(B9) is exactly the memory-less condition in Theorem 1, and therefore  $\tau_j$  follows an exponential distribution with the  $\lambda_j$  determined by the current state  $X_j$ . As a consequence of the embedded discrete Markov chain and the exponential distribution holding time, a quantum *continuous Markov process* state can be prepared as follows:  $n \lceil \log S \rceil$  qubits are introduced for the storage of the discrete Markov chain, and another  $n \lceil \log(-\frac{1}{\lambda_{\min}} \ln \epsilon) \rceil$  qubits are introduced for the holding time  $\tau_j$ . The initial state  $|X_1\rangle = \sum_{k=1}^S p(k) |k\rangle$  is derived by  $S$  control-rotation gates via Grover's state preparation method. Following that,  $n - 1$  successive transition matrix operators, each of which consists of  $S^2$  multi-controlled rotation gates, are applied to generate  $|X_j\rangle : 2 \leq j \leq n$ . The  $n$  holding times can be prepared parallel, and each  $\tau_j$  needs at most  $s$  different exponential distribution with  $S \lceil \log(-\frac{1}{\lambda_{\min}} \ln \epsilon) \rceil$  gates and  $S$  circuit depth. In summary, the total number of gates is  $S + (n - 1) * S^2 + n * S \lceil \log(-\frac{1}{\lambda_{\min}} \ln \epsilon) \rceil = O(nS \lceil S + \log(-\frac{\ln \epsilon}{\lambda_{\min}}) \rceil)$ , and the circuit depth is  $S + (n - 1) * S^2 + n * S = O(nS^2)$ .  $\square$

### 5. Proof of Theorem 6

*Proof.* As shown in FIG. 6, the preparation can be divided into two steps: Firstly, the stochastic process of intensity  $\lambda(t)$  is prepared on parallel  $n * q_{\mathcal{F}}$  qubits, and the circuit depth is  $O(d_{\mathcal{F}})$  as given. Secondly, the holding time  $\tau_j$  is prepared by a sequence of controlled- $V$  operators. Given a piece of Cox process and the corresponding fixed intensity  $\lambda$ , the holding time follows an exponential distribution as described in Theorem 1 so that it can be prepared within 1 circuit depth by rotation angles  $\theta_j = \tilde{\epsilon}^{1/2^{j+1}} : 1 \leq j \leq m$ , where  $\tilde{\epsilon} = e^{-\lambda T}$ . As for varying digital-encoded  $\lambda = |l_1, l_2, \dots, l_{q_{\mathcal{F}}}\rangle$ , it can be divided into  $2_{q_{\mathcal{F}}}$  sequences of controlled-rotation gates with  $2_{q_{\mathcal{F}}}$  circuit depth. Hence the total circuit depth for preparing  $\tau_j$  is  $d_{\mathcal{F}} + 2_{q_{\mathcal{F}}}$ . On the other hand, the preparation of increments  $Y_j$  can be implemented parallel with  $d_{\mathcal{G}}$  circuit depth. Thus the circuit depth of the preparation is  $\max\{d_{\mathcal{F}} + 2_{q_{\mathcal{F}}}, d_{\mathcal{G}}\}$ . To derive  $X_j$  or  $T_j$ ,  $n$  adders are needed, with  $nd_{\mathcal{G}}$  or  $-\frac{n \ln \epsilon}{\lambda_{\min}}$ , respectively.  $\square$

## Appendix C: Proofs for Information Extraction Problem

### 1. Proof of Theorem 7

*Proof.* A direct computation shows that:

$$I(X, T) = \int_{t=0}^T X(t) dt = \sum_{j=0}^n X_j \tau_j. \quad (\text{C1})$$

The expected value of Eq.(C1) is evaluated as:

$$\begin{aligned} \mathbb{E}[f(I(X, T))] &= \sum_{X(t) \in \bar{\Omega}_n} f\left(\int_{t=0}^T X(t) dt\right) \mathbb{P}[X(t)] \\ &= \sum_{X(t) \in \bar{\Omega}_n} f\left(\sum_{j=0}^n X_j \tau_j\right) \mathbb{P}[X(t)] \\ &= \sum_{X(t) \in \bar{\Omega}_n} f\left(\sum_{j=0}^n Z_j\right) \mathbb{P}[X(t)], \end{aligned} \quad (\text{C2})$$

where  $Z_j = X_j \tau_j$  can be derived via a quantum multiplication circuit introduced in Lemma 9 with complexity  $O(l_x l_\tau)$ . The total circuit depth is  $O(P + nl_x l_\tau)$  (as shown in FIG. 7 (c)). Noticing that the variables of  $f$  in Eq.(C2) can be evaluate through a standard procedure (one can see [27] for reference). To guarantee the theoretical closure, we shall sketch this procedure as follows. Suppose that the function  $f$  can be truncated on an interval of length  $P$ , then it can be extended to a  $P$ -periodic function  $f_P$ . The Fourier approximation of order  $L$  for  $f_P$  is denoted by  $f_{P,L}(x) = \sum_{l=-L}^L c_l e^{i \frac{2\pi l}{P} x}$ , then Eq.(C2) is evaluated as

$$\begin{aligned} \mathbb{E}[f_{P,L}(I(X, T))] &= \mathbb{E}[f_{P,L}\left(\sum_{j=0}^n Z_j\right)] \\ &= \sum_{l=-L}^L c_l \mathbb{E}[e^{i \frac{2\pi l}{P} (\sum_{j=0}^n Z_j)}] \\ &= \sum_{l=-L}^L c_l (\mathbb{E}[\cos\left(\frac{2\pi l}{P} (\sum_{j=0}^n Z_j)\right)] + i \mathbb{E}[\sin\left(\frac{2\pi l}{P} (\sum_{j=0}^n Z_j)\right)]), \end{aligned} \quad (\text{C3})$$

Each term  $\mathbb{E}[\cos\left(\frac{2\pi l}{P} (\sum_{j=0}^n Z_j)\right)]$  and  $\mathbb{E}[\sin\left(\frac{2\pi l}{P} (\sum_{j=0}^n Z_j)\right)]$  in Eq.(C3) can be evaluated via the standard amplitude estimation algorithm. Given the error bound  $\epsilon$ , the circuit should be repeated  $O(1/\epsilon)$  times for each term. The total time complexity is hence  $O\left(\frac{LP}{\epsilon} (P + nl_x l_\tau)\right)$   $\square$

### 2. Proof of Theorem 8

*Proof.* A direct computation shows that:

$$\begin{aligned} J(X, T) &= \int_{t=0}^T g(t) X(t) dt \\ &= \sum_{j=1}^n X_j G_j \\ &= \sum_{j=1}^n \left(\sum_{j'=1}^j Y_{j'}\right) G_j \end{aligned}$$

where  $G_j = \int_{T_{j-1}}^T g(t) dt$  is a piece-wise integral on the interval  $[T_{j-1}, T]$  with  $T_j = \sum_{j'=1}^j \tau_{j'}$  and  $T_0 = 0$ , and  $Y_{j'}$  is the  $j'^{th}$  increment. By exchanging the order of summation, one has that:

$$\begin{aligned} J(X, T) &= \sum_{j'=1}^n Y_{j'} \left(\sum_{j=j'}^n G_j\right) \\ &= \sum_{j'=1}^n Y_{j'} F(T - T_{j'-1}) \end{aligned} \quad (\text{C4})$$

$$= \sum_{j'=1}^n Y_{j'} G(T_{j'-1}), \quad (\text{C5})$$

where  $F(T') = \int_{T-T'}^T g(t) dt$  in Eq.(C4) satisfies:

$$F(T - T_{j'-1}) = \int_{T_{j'-1}}^T g(t) dt = \sum_{j=j'}^n G_j,$$

and  $G(T') = \int_{T'}^T g(t) dt$  in Eq.(C5) satisfies:

$$G(T_{j'-1}) = \int_{T_{j'-1}}^T g(t) dt = \sum_{j=j'}^n G_j.$$

Thus the expected value of Eq.(C4) and Eq.(C5) can be evaluated as

$$\begin{aligned} \mathbb{E}[f(J(X, T))] &= \sum_{X(t) \in \bar{\Omega}_n} f\left(\sum_{j=1}^n Y_j F(T - T_{j-1})\right) \mathbb{P}[X(t)] \end{aligned} \quad (\text{C6})$$

$$= \sum_{X(t) \in \bar{\Omega}_n} f\left(\sum_{j=1}^n Y_j G(T_{j-1})\right) \mathbb{P}[X(t)] \quad (\text{C7})$$

$$= \sum_{X(t) \in \bar{\Omega}_n} f\left(\sum_{j=1}^n W_j\right) \mathbb{P}[X(t)]. \quad (\text{C8})$$

The state  $F(T - T_{j'-1})$  in Eq.(C6) is a function of the variable  $T - T_{j'-1}$ , and hence can be computed via a operator  $F$  on the  $T - T_{j'-1}$  qubit as illustrated in FIG.

**7 (d).** And the directed area  $W_j = Y_j F(T - T_{j'-1})$  can be derived through a quantum multiplier introduced in Lemma 9 with complexity  $O(l_x l_\tau)$ . In the same way the state  $G(T_{j'-1})$  in Eq.(C7) is a function of the variable  $T_{j'-1}$ , and hence can be computed via a operator  $G$  on the  $T_{j'-1}$  qubit. And the directed area  $W_j = Y_j G(T_{j'-1})$  can be derived with complexity  $O(l_Y l_T)$  (see FIG. 7 (e) for reference). The total circuit depth is  $O(\mathcal{P} + \mathcal{F} + nl_x l_\tau + n \max(l_x, l_\tau))$  or  $O(\mathcal{P} + \mathcal{G} + nl_Y l_T)$ . Noticing that the expression in Eq.(C8) once again take the form of a summation, and thus can be solved through a standard procedure of amplitude estimation as mentioned above: The Fourier approximation of order  $L$  for  $f_P$  is denoted by  $f_{P,L}(x) = \sum_{l=-L}^L c_l e^{i \frac{2\pi l}{p} x}$ , then Eq.(C8) is evaluated

as

$$\begin{aligned} \mathbb{E}[f_{P,L}(J(X, T))] &= \mathbb{E}[f_{P,L}(\sum_{j=1}^n W_j)] \\ &= \sum_{l=-L}^L c_l \mathbb{E}[e^{i \frac{2\pi l}{p} (\sum_{j=1}^n W_j)}] \\ &= \sum_{l=-L}^L c_l (\mathbb{E}[\cos(\frac{2\pi l}{p} (\sum_{j=1}^n W_j))] + i \mathbb{E}[\sin(\frac{2\pi l}{p} (\sum_{j=1}^n W_j))]). \end{aligned} \quad (\text{C9})$$

Each term  $\mathbb{E}[\cos(\frac{2\pi l}{p} (\sum_{j=1}^n W_j))]$  and  $\mathbb{E}[\sin(\frac{2\pi l}{p} (\sum_{j=1}^n W_j))]$  in Eq.(C9) can be evaluated via rotation operators on the target qubit controlled by  $W_j$  together with a standard amplitude estimation subcircuit.(as shown in the box in FIG. 7 (d) and FIG. 7 (e)). Given the error bound  $\epsilon$ , the circuit should be repeated  $O(1/\epsilon)$  times for each term. The total time complexity is hence  $O(\frac{LP}{\epsilon}(\mathcal{P} + \mathcal{F} + nl_x l_\tau + n \max(l_x, l_\tau)))$  or  $O(\frac{LP}{\epsilon}(\mathcal{P} + \mathcal{G} + nl_Y l_T))$  for holding time and increment representation, respectively.  $\square$

- 
- [1] A. Papantoleon, arXiv preprint arXiv:0804.0482 (2008).
- [2] O. E. Barndorff-Nielsen, T. Mikosch, and S. I. Resnick, *Lévy processes: theory and applications* (Springer Science & Business Media, 2001).
- [3] T. M. Liggett, *Continuous time Markov processes: an introduction*, Vol. 113 (American Mathematical Soc., 2010).
- [4] W. J. Anderson, *Continuous-time Markov chains: An applications-oriented approach* (Springer Science & Business Media, 2012).
- [5] A. Dassios and J.-W. Jang, *Finance and Stochastics* **7**, 73 (2003).
- [6] S. M. Ross, J. J. Kelly, R. J. Sullivan, W. J. Perry, D. Mercer, R. M. Davis, T. D. Washburn, E. V. Sager, J. B. Boyce, and V. L. Bristow, *Stochastic processes*, Vol. 2 (Wiley New York, 1996).
- [7] Y. V. Kozachenko, O. O. Pogorilyak, I. V. Rozora, and A. M. Tegza, *Simulation of stochastic processes with given accuracy and reliability* (Elsevier, 2016).
- [8] R. P. Feynman, *Optics news* **11**, 11 (1985).
- [9] D. P. DiVincenzo, *Fortschritte der Physik: Progress of Physics* **48**, 771 (2000).
- [10] F. Arute, K. Arya, R. Babbush, D. Bacon, J. C. Bardin, R. Barends, R. Biswas, S. Boixo, F. G. Brandao, D. A. Buell, *et al.*, *Nature* **574**, 505 (2019).
- [11] R. Orus, S. Mugel, and E. Lizaso, *Reviews in Physics* **4**, 100028 (2019).
- [12] D. J. Egger, C. Gambella, J. Marecek, S. McFaddin, M. Mevissen, R. Raymond, A. Simonetto, S. Woerner, and E. Yndurain, *IEEE Transactions on Quantum Engineering* (2020).
- [13] D. Herman, C. Googin, X. Liu, A. Galda, I. Safro, Y. Sun, M. Pistoia, and Y. Alexeev, arXiv preprint arXiv:2201.02773 (2022).
- [14] S. McArdle, S. Endo, A. Aspuru-Guzik, S. C. Benjamin, and X. Yuan, *Reviews of Modern Physics* **92**, 015003 (2020).
- [15] C. Outeiral, M. Strahm, J. Shi, G. M. Morris, S. C. Benjamin, and C. M. Deane, *Wiley Interdisciplinary Reviews: Computational Molecular Science* **11**, e1481 (2021).
- [16] P. S. Emani, J. Warrell, A. Anticevic, S. Bekiranov, M. Gandal, M. J. McConnell, G. Sapiro, A. Aspuru-Guzik, J. T. Baker, M. Bastiani, *et al.*, *Nature Methods*, 1 (2021).
- [17] H. Ma, M. Govoni, and G. Galli, *npj Computational Materials* **6**, 1 (2020).
- [18] Y. Cao, J. Romero, and A. Aspuru-Guzik, *IBM Journal of Research and Development* **62**, 6 (2018).
- [19] M. Schuld and F. Petruccione, *Supervised learning with quantum computers*, Vol. 17 (Springer, 2018).
- [20] L. Grover and T. Rudolph, arXiv preprint quant-ph/0208112 (2002).
- [21] A. C. Vazquez and S. Woerner, *Physical Review Applied* **15**, 034027 (2021).
- [22] A. G. Rattew and B. Koczor, arXiv preprint arXiv:2205.00519 (2022).
- [23] T. J. Elliott and M. Gu, *npj Quantum Information* **4** (2018).
- [24] T. J. Elliott, A. J. Garner, and M. Gu, *New Journal of Physics* **21**, 013021 (2019).
- [25] T. J. Elliott, *PRX Quantum* **2**, 020342 (2021).
- [26] K. Korzekwa and M. Lostaglio, *Physical Review X* **11**, 021019 (2021).
- [27] A. Montanaro, *Proceedings of the Royal Society A: Mathematical, Physical and Engineering Sciences* **471**,

- 20150301 (2015).
- [28] P. Rebentrost, B. Gupt, and T. R. Bromley, *Physical Review A* **98**, 022321 (2018).
- [29] N. Stamatopoulos, D. J. Egger, Y. Sun, C. Zoufal, R. Iten, N. Shen, and S. Woerner, *Quantum* **4**, 291 (2020).
- [30] A. Martin, B. Candelas, Á. Rodríguez-Rozas, J. D. Martín-Guerrero, X. Chen, L. Lamata, R. Orús, E. Solano, and M. Sanz, arXiv preprint arXiv:1904.05803 (2019).
- [31] S. Woerner and D. J. Egger, *npj Quantum Information* **5**, 1 (2019).
- [32] C. Blank, D. K. Park, and F. Petruccione, *npj Quantum Information* **7**, 1 (2021).
- [33] V. Giovannetti, S. Lloyd, and L. Maccone, *Physical review letters* **100**, 160501 (2008).
- [34] V. Giovannetti, S. Lloyd, and L. Maccone, *Physical Review A* **78**, 052310 (2008).
- [35] F.-Y. Hong, Y. Xiang, Z.-Y. Zhu, L.-Z. Jiang, and L.-N. Wu, *Physical Review A* **86**, 010306 (2012).
- [36] D. Lando, *Review of Derivatives research* **2**, 99 (1998).
- [37] R. C. Merton, *The American Economic Review* **88**, 323 (1998).
- [38] Y.-K. Kwok, *Mathematical models of financial derivatives* (Springer Science & Business Media, 2008).
- [39] F. Black and M. Scholes, in *World Scientific Reference on Contingent Claims Analysis in Corporate Finance: Volume 1: Foundations of CCA and Equity Valuation* (World Scientific, 2019) pp. 3–21.
- [40] R. C. Merton, *Journal of financial economics* **3**, 125 (1976).
- [41] H. U. Gerber and E. S. Shiu, *North American Actuarial Journal* **2**, 48 (1998).
- [42] M. B. Garman, *Journal of financial Economics* **3**, 257 (1976).
- [43] A. Madhavan, *Journal of financial markets* **3**, 205 (2000).
- [44] H. U. Gerber and E. S. Shiu, *Insurance: Mathematics and Economics* **24**, 3 (1999).
- [45] S. A. Cuccaro, T. G. Draper, S. A. Kutin, and D. P. Moulton, arXiv preprint quant-ph/0410184 (2004).